SIAM J. NUMER. ANAL.
Vol. 57, No. 4, pp. 1574–1601

THE L^2-NORM STABILITY ANALYSIS OF RUNGE–KUTTA DISCONTINUOUS GALERKIN METHODS FOR LINEAR HYPERBOLIC EQUATIONS*

YUAN XU†, QIANG ZHANG†, CHI-WANG SHU‡, AND HAIJIN WANG§

Abstract. In this paper we propose a simple and unified framework to investigate the L^2-norm stability of the explicit Runge–Kutta discontinuous Galerkin (RKDG) methods when solving the linear constant-coefficient hyperbolic equations. Two key ingredients in the energy analysis are the temporal differences of numerical solutions in different Runge–Kutta stages and a matrix transferring process. Many popular schemes, including the fourth order RKDG schemes, are discussed in this paper to show that the presented technique is flexible and useful. Different performances in the L^2-norm stability of different RKDG schemes are carefully investigated. For some lower-degree piecewise polynomials, the monotonicity stability is proved if the stability mechanism can be provided by the upwind-biased numerical fluxes. Some numerical examples are also given.

Key words. Runge–Kutta discontinuous Galerkin method, explicit time-marching, energy analysis, L^2-norm stability

AMS subject classifications. 65M12, 65M60

DOI. 10.1137/18M1230700

1. Introduction. In this paper we propose an analysis framework to obtain the L^2-norm stability of the explicit Runge–Kutta discontinuous Galerkin (RKDG) methods when solving the linear constant-coefficient conservation law

$$U_t + \beta U_x = 0, \quad x \in I = (0,1), \quad t > 0, \tag{1.1}$$

which is, for simplicity, subject to the periodic boundary condition. Here $U(x,t)$ is the unknown solution and $\beta \neq 0$ is a given constant. In this paper we would like to take the one-dimensional scalar equations as an example. One-dimensional systems can be treated in the same way by diagonalization. The multidimensional case is also similar, with the main difference coming from the inverse properties of the discontinuous finite element spaces.

After the first version of the discontinuous Galerkin (DG) method was introduced in 1973 by Reed and Hill [22], in the framework of neutron linear transport, the DG method has been the focus of intensive research, because it has many advantages. For example, this method has strong stability and optimal accuracy and can capture discontinuous jumps sharply. It combines the advantages of finite element methods

*Received by the editors December 5, 2018; accepted for publication (in revised form) April 24, 2019; published electronically July 3, 2019.
https://doi.org/10.1137/18M1230700
Funding: The work of the first, second, and fourth authors was supported by the National Natural Science Foundation of China grant 11671199. The work of the first and second authors was supported by the National Natural Science Foundation of China grant 11571290. The work of the third author was supported by ARO grant W911NF-16-1-0103 and National Science Foundation grant DMS-1719410. The work of the fourth author was supported by the National Natural Science Foundation of China grant 11601241 and the Natural Science Foundation of Jiangsu Province grant BK20160877.
†Department of Mathematics, Nanjing University, Nanjing 210093, Jiangsu Province, China (dz1721005@smail.nju.edu.cn, qzh@nju.edu.cn).
‡Division of Applied Math, Brown University, Providence, RI 02912-0001 (shu@dam.brown.edu).
§College of Science, Nanjing University of Posts and Telecommunications, Nanjing 210023, Jiangsu Province, China (hjwang@njupt.edu.cn).

and finite volume methods. An important development in the DG method was carried out in the late 1980s, when Cockburn et al. [4, 5, 6, 7, 8] combined the explicit Runge–Kutta time-marching and the DG spatial discretization to form the RKDG schemes. There have been many published papers in this field since then; see, for example, the review papers [3, 9] and the references therein.

Compared with the wide applications of RKDG methods, there is relatively less work on the theory, for example, on the numerical stability in a suitable norm, which is an important issue for the reliability of the scheme. Related to the semidiscrete DG method for nonlinear conservation laws, the well-known conclusion is the local cell entropy inequality, given by Jiang and Shu [16], which implies that the L^2-norm of the numerical solution does not increase with time. The stability mechanism provided by the spatial DG discretization is very weak; hence the explicit time-marching to the DG method must be treated carefully if the time step is assumed to only satisfy the standard Courant–Friedrichs–Lewy (CFL) condition that the ratio of the time step over the spatial mesh size is upper bounded by a constant. For example, the Euler-forward time-marching to the DG method is linearly unstable under the standard CFL condition for any polynomial degree $k \geq 1$. To overcome this difficulty, one successful treatment is to adopt the explicit total-variation-diminishing Runge–Kutta time-marching [23]; please refer to the series of papers by Cockburn et al. [4, 5, 6, 7, 8]. This type of time-marching has been later termed *strong-stability-preserving* (SSP) [13], which is widely applied in the analysis of nonlinear stability including the total-variation-diminishing in the means (TVDM) property [3] and the positivity-preserving property [30] for nonlinear conservation laws.

In this paper we focus on the fully discrete RKDG methods for linear constant-coefficient hyperbolic equations and would like to establish a general framework for analyzing their L^2-norm stability. We start by noting that this analysis cannot follow the SSP framework [13, Lemma 2.1] because the RKDG method does not satisfy the basic assumption that the Euler-forward time-marching in each stage of evolution is stable under the standard CFL condition. Thus the high-order Runge–Kutta time discretization must be analyzed directly. There are two main strategies to do this analysis. The easier strategy is to carry out a Fourier analysis [14, 19, 31], which might give the sharp CFL condition. However, this technique demands many assumptions, for example, uniform meshes and the periodic boundary condition, and, if only eigenvalues of the amplification matrices are considered, it would also require the spatial discretization operator to be normal. This technique is also difficult to generalize to nonuniform meshes, nonperiodic boundary conditions, linear variable-coefficient problems, nonlinear problems, and multidimensional problems [17]. Therefore, we would like in this paper to follow the second strategy, which is the so-called energy analysis to overcome the above difficulties. The motivation comes from the analysis of the optimal error estimates for two RKDG methods to solve nonlinear conservation laws carried out in [28, 29], which is obtained by virtue of suitable projections and the stability analysis for the linear case.

In this paper we develop the technique initialized in [28, 29] to any RKDG(s, r, k) method with stage s and order r (in time-marching), as well as with polynomial degree k in the spatial DG discretization. The main treatment in the stability analysis is to establish a good energy equation to clearly reflect the evolution of the L^2-norm of the numerical solution and to explicitly show the stability mechanism hidden in the fully discrete scheme. For this purpose, we follow the original idea in [28, 29] and make the following important developments in this paper:

1. The first development is the temporal differences of the numerical solution

in different Runge–Kutta stages (sometimes referred to more briefly as the "stage solutions" below), which are related to different orders of time derivatives. These temporal differences are easily defined by induction, and their treatment is not limited to one-step time-marching. In fact, we combine multiple steps in the time-marching, with possibly different time step sizes as well. See sections 3 and 5.3 for more details.

2. The second development is the simple matrix transferring process, which enables us to transform an ordinary energy equation to a particular energy equation in our desired form. In this transferring process, the temporal differences of stage solutions play a very important role, and some general properties of the DG spatial discretization are also implicitly used. After the transferring process, we can obtain the expected stability conclusion by looking at a termination index ζ and a contribution index ρ, as defined and discussed in section 3. These indices explicitly reflect the stability mechanism of the RKDG method; hence they are very useful in analyzing different stabilities for fully discrete RKDG methods.

This general framework, which heavily uses various temporal differences of the DG numerical solution in different Runge–Kutta stages, might turn out to be useful for future generalizations to linear variable coefficient and nonlinear problems. Furthermore, our line of analysis is very convenient and useful for obtaining optimal error estimates of the RKDG method, as has been done in [29] and [20]. We believe that this technique works well for many numerical methods to solve (almost) skew-symmetric problems.

We point out related earlier work in [18, 24, 26] for the stability of Runge–Kutta time discretizations for seminegative spatial operators with temporal accuracy up to fourth order. Levy and Tadmor [18] used the energy method to prove, for coercive problems, the monotonicity stability of some fully discrete schemes with Runge–Kutta time-marching of order $r = 3, 4$ (please see section 2 for the definition of monotonicity stability). After that, this result was extended to the general linear Runge–Kutta time-marching, and the SSP framework [13] was utilized. However, the RKDG methods for the hyperbolic problems are not strongly coercive, and the SSP framework is not suitable for their L^2-norm stability analysis. In 2002, Tadmor [26] proved the monotonicity stability of the three-stage third order Runge–Kutta time discretization with any seminegative linear spatial operator, including the RKDG$(3, 3, k)$ method, without the coercive assumption, and posed the monotonicity stability of the four-stage fourth order Runge–Kutta time discretization with a seminegative linear spatial operator, including the RKDG$(4, 4, k)$ method, as an open problem. In 2010, Zhang and Shu [29] and Burman, Ern, and Fernández [1] independently proved the monotonicity stability and error estimates for the RKDG$(3, 3, k)$ method, along different analysis lines. The open problem proposed by Tadmor [26] has been partly answered by Sun and Shu [24] in 2017 by a simple counterexample that the four-stage fourth order Runge–Kutta time discretization with a seminegative linear spatial operator does not always have the monotonicity stability. However, the L^2-norm of the solution is proved to have the monotonicity property after every two time steps. Notice that the seminegative linear operator in the counterexample in [24] is *not* the DG operator; hence the result in [24] does not answer the question of whether the RKDG$(4, 4, k)$ method has the monotonicity stability or not. In this paper, we use numerical examples (see Example 1 in section 6) to show that the monotonicity stability does not hold for the first time step of the RKDG$(4, 4, k)$ method. Actually, the destruction of the monotonicity can happen at any time level. Using our analysis technique, we suc-

cessfully recover the conclusions in [24] and prove in addition that the L^2-norm of the numerical solution is monotone after every three steps, which implies the strong stability (please see section 2 for the definition of strong stability) of the RKDG$(4,4,k)$ method after the second time step. Very recently, Sun and Shu [25] extended their earlier work in [24] by developing a general framework for analyzing the stability of Runge–Kutta time-marching for seminegative linear spatial operators. Some of the results obtained in our paper overlap with the results in [25]; however, we concentrate on the particular DG spatial operator and use its properties explicitly, and hence we are able to obtain some results not covered in [25]. The lines of analysis in our paper and in [25] are also very different.

The content of this paper is organized as follows. In section 2, we first present the general construction of the RKDG methods and state the L^2-norm stability of the RKDG(r,r,k) methods for any degree $k \geq 0$ and $1 \leq r \leq 12$. Also, weak(γ) stability, strong (boundedness) stability, and monotonicity stability are defined in this section. In section 3 we present the framework for our analysis, including the temporal differences of solutions in different stages, the matrix transferring process, and two important indices. In section 4 the above discussion is applied to four classical RKDG methods from the first order to the fourth order in time. Some important remarks and extensions are given in section 5. Numerical examples are given in section 6, and concluding remarks are given in section 7.

2. RKDG method and the main result. In this section we would like to present the RKDG method under consideration, expressed in the Shu–Osher form [23].

2.1. Discontinuous finite element space. Let $\{I_j\}_{j=1}^J$ be a quasi-uniform partition of I, where each element $I_j = (x_{j-1/2}, x_{j+1/2})$ has length $h_j = x_{j+1/2} - x_{j-1/2}$. The maximum length of elements is denoted by $h = \max_{j=1,2,\ldots,J} h_j$. The discontinuous finite element space is defined as

$$V_h = \{v \in L^2(I) : v|_{I_j} \in \mathcal{P}^k(I_j),\ j = 1, \ldots, J\}, \tag{2.1}$$

where $\mathcal{P}^k(I_j)$ denotes the space of polynomials in I_j of degree at most $k \geq 0$. Note that the functions in V_h are allowed to have discontinuities across element interfaces. Following [2], the jump and weighted average are respectively denoted by

$$[\![v]\!]_{j+\frac{1}{2}} = v^+_{j+\frac{1}{2}} - v^-_{j+\frac{1}{2}} \quad \text{and} \quad \{\!\{v\}\!\}^{(\theta)}_{j+\frac{1}{2}} = \theta v^-_{j+\frac{1}{2}} + (1-\theta) v^+_{j+\frac{1}{2}}, \tag{2.2}$$

where $v^{\pm}_{j+1/2}$ are traces along different directions at the point $x_{j+1/2}$, and θ is the given weight.

2.2. Semidiscrete scheme. Following the notation of [20, 29], the semidiscrete DG method of (1.1) is defined as follows: find the map $u\colon [0,T] \to V_h$ such that

$$(u_t, v) = \mathcal{H}(u, v) \quad \forall\, v \in V_h, \quad t \in (0,T], \tag{2.3}$$

subject to the initial solution $u(x,0) \in V_h$. Here $(\cdot,\cdot)$ is the standard inner product in $L^2(I)$, with the associated L^2-norm $\|\cdot\|$, and

$$\mathcal{H}(u,v) = \sum_{1 \leq j \leq J} \left[\int_{I_j} \beta u v_x \, \mathrm{d}x + \beta \{\!\{u\}\!\}^{(\theta)}_{j+\frac{1}{2}} [\![v]\!]_{j+\frac{1}{2}} \right] \tag{2.4}$$

is the spatial DG discretization. We would assume $\beta(\theta - 1/2) > 0$ in this paper, such that $\hat{f}(u^-, u^+) \equiv \beta \{\!\{u\}\!\}^{(\theta)}$ forms an upwind-biased numerical flux at each element

interface. Actually, $\hat{f}(u^-, u^+)$ is just the purely upwind flux when $\theta = 0$ for $\beta < 0$, and $\theta = 1$ for $\beta > 0$.

It is worth mentioning that the periodic boundary condition has been used in the above definition. Other boundary conditions can be treated in a similar way. For example, please refer to [27] for the inflow boundary condition.

Remark 2.1. In general, $u(x, 0)$ is given as the approximation of the given initial solution. For example, the L^2-projection is frequently used in practice. In this paper we will not discuss this issue, since the initial solution only affects the error, but not the stability.

2.3. Fully discrete scheme. In the fully discrete method, we would like to seek the numerical solution u^n at time levels $t^n = n\tau$, where τ is the time step. The time step could actually change from step to step. For simplicity, in this paper we take it as a constant unless otherwise stated.

By virtue of the Shu–Osher representation [23], the general construction of the RKDG(s, r, k) method is given as follows. For $\ell = 0, 1, \ldots, s-1$, the stage solutions, advancing from t^n to t^{n+1}, are successively sought by the variational formula

$$(u^{n,\ell+1}, v) = \sum_{0 \le \kappa \le \ell} \Big[c_{\ell\kappa}(u^{n,\kappa}, v) + d_{\ell\kappa}\tau \mathcal{H}(u^{n,\kappa}, v) \Big] \quad \forall v \in V_h, \tag{2.5}$$

where $d_{\ell\ell} \neq 0$. Here $u^{n,0} = u^n$ and $u^{n+1} = u^{n,s}$.

There are plenty of examples in the review paper [11]. In this paper we would like to start from the RKDG(r, r, k) method whose number of stages s is equal to the order r. For the linear constant-coefficient problem, all Runge–Kutta methods with the same number of stages and order are equivalent [13]. Under the SSP framework, the coefficients in (2.5) of this method can be written in two matrices,

$$\{c_{\ell\kappa}\} = \left[\begin{array}{ccc:c} 1 & & & \\ & \ddots & & \\ & & 1 & \\ \hdashline g_{r-1,0} & \cdots & g_{r-1,r-2} & g_{r-1,r-1} \end{array}\right], \quad \{d_{\ell\kappa}\} = \left[\begin{array}{ccc:c} 1 & & & \\ & \ddots & & \\ & & 1 & \\ \hdashline & & & g_{r-1,r-1} \end{array}\right],$$

where the row (and column) numbers are both taken from $\{0, 1, 2, \ldots, r-1\}$. The parameters are defined as follows. Let $g_{0,0} = 1$, and recursively define for $r \ge 2$ that

$$g_{r-1,\ell} = \frac{1}{\ell} g_{r-2,\ell-1}, \quad \ell = 1, 2, \ldots, r-2,$$

with $g_{r-1,r-1} = 1/r!$ and $g_{r-1,0} = 1 - \sum_{\ell=1}^{r-1} g_{r-1,\ell}$. The related coefficients for $r \le 8$ are listed in Table 1 [13, Table 3.1].

Remark 2.2. Only for homogeneous linear problems, both SSP and non-SSP Runge–Kutta methods of s stages with sth order accuracy are identical. This is not true for the general linear and nonlinear problems. It is a well-known conclusion [12] that there does not exist any SSP Runge–Kutta scheme of four stages with fourth order accuracy for nonlinear problems.

2.4. Main result. Denote by $\lambda = |\beta|\tau h^{-1}$ the CFL number. To clearly state the L^2-norm stability of the RKDG methods, we would like to adopt three different stability concepts in this paper. They are given as follows.

TABLE 1
Coefficients of the RKDG(r, r, k) methods.

r	$g_{r-1,0}$	$g_{r-1,1}$	$g_{r-1,2}$	$g_{r-1,3}$	$g_{r-1,4}$	$g_{r-1,5}$	$g_{r-1,6}$	$g_{r-1,7}$
1	1							
2	$\frac{1}{2}$	$\frac{1}{2}$						
3	$\frac{1}{3}$	$\frac{1}{2}$	$\frac{1}{6}$					
4	$\frac{3}{8}$	$\frac{1}{3}$	$\frac{1}{4}$	$\frac{1}{24}$				
5	$\frac{11}{30}$	$\frac{3}{8}$	$\frac{1}{6}$	$\frac{1}{12}$	$\frac{1}{120}$			
6	$\frac{53}{144}$	$\frac{11}{30}$	$\frac{3}{16}$	$\frac{1}{18}$	$\frac{1}{48}$	$\frac{1}{720}$		
7	$\frac{103}{280}$	$\frac{53}{144}$	$\frac{11}{60}$	$\frac{3}{48}$	$\frac{1}{72}$	$\frac{1}{240}$	$\frac{1}{5040}$	
8	$\frac{2119}{5760}$	$\frac{103}{280}$	$\frac{53}{288}$	$\frac{11}{180}$	$\frac{1}{64}$	$\frac{1}{360}$	$\frac{1}{1140}$	$\frac{1}{40320}$

1. *Weak(γ) stability.* There exists an integer $\gamma \geq 2$, such that
$$\|u^{n+1}\|^2 \leq (1 + C\lambda^\gamma)\|u^n\|^2, \quad n \geq 0, \tag{2.6}$$
if the CFL number λ is small enough, where the constant $C > 0$ is independent of τ, h, and n. As a result, the RKDG method is generally stable with the exponent-type constant, provided that λ^γ/τ is bounded.
2. *Strong (boundedness) stability.* There exists an integer n_*, such that
$$\|u^n\| \leq \|u^0\|, \quad n \geq n_*, \tag{2.7}$$
if the CFL number λ is small enough.
3. *Monotonicity stability.* There holds $\|u^{n+1}\| \leq \|u^n\|$ for $n \geq 0$ if the CFL number λ is small enough. Obviously, monotonicity stability implies the strong (boundedness) stability. Note that our monotonicity stability is sometimes called strong stability in the literature.

It is worth mentioning the following facts. If the weak(γ) stability cannot be strengthened to the other two stabilities, the scheme might be linearly unstable for any fixed CFL number, no matter how small it is. If both the weak(γ) stability and the strong (boundedness) stability hold, the scheme is obviously stable under the standard CFL condition.

In the following theorem we present the L^2-norm stability results for some popular RKDG methods.

THEOREM 2.1. *For the RKDG(r, r, k) methods, with $1 \leq r \leq 12$ and arbitrary k, the stability conclusion strongly depends on the remainder when r is divided by 4, namely,*

$r \mod 4$	0	1	2	3
stability type	*strong*	*weak(r + 1)*	*weak(r + 2)*	*monotonicity*

To conclude this section, we would like to make some remarks below.

Remark 2.3. If the RKDG(r, r, k) method is weakly stable, a stronger constraint on the time step size is needed to ensure the general stability. Theorem 2.1 shows that $\tau = \mathcal{O}(h^{\frac{r+1}{r}})$ is sufficient for $r \equiv 1 \pmod 4$, and $\tau = \mathcal{O}(h^{\frac{r+2}{r+1}})$ for $r \equiv 2 \pmod 4$. This conclusion generalizes the result in [10, Theorem 3.2] for the even-order time-marching, in which the strictly skew-symmetric property (see section 3, which implies that the spatial operator is normal) for the spatial discretization is required. In this paper, we only require an approximate skew-symmetric property (which could be a nonnormal operator) as specified in section 3.

3. Stability analysis. In this section we present the line of analysis to obtain the L^2-norm stability of any RKDG methods. It is based on the energy technique and mainly includes two components. Below we will use the generalized notations

$$u^{n,\kappa+ms} = u^{n+m,\kappa}, \quad \kappa = 0, 1, \ldots, s-1, \tag{3.1}$$

for any given integer $m \geq 1$. Here n and $n+m$ are called the time levels, κ and $\kappa+ms$ are called the stage numbers, and m is called the step number. In many cases, we take $m = 1$.

3.1. Preliminaries. Now we recall some preliminary conclusions that will be used below. If the proofs are trivial, we will omit them.

3.1.1. Inverse inequity and discrete trace inequity of the finite element space. For any function $v \in V_h$, there exists an inverse constant μ independent of h and v, such that

$$\|v_x\| \leq \mu h^{-1} \|v\|, \qquad \text{(inverse inequity)} \tag{3.2a}$$

$$\|v\|_{\Gamma_h} \leq \mu h^{-1/2} \|v\|, \qquad \text{(discrete trace inequity)} \tag{3.2b}$$

where $\|v\|$ is the L^2-norm as usual, and

$$\|v_x\| = \left\{ \sum_{1 \leq j \leq J} \int_{I_j} (v_x)^2 \, \mathrm{d}x \right\}^{\frac{1}{2}}, \quad \|v\|_{\Gamma_h} = \left\{ \sum_{1 \leq j \leq J} \frac{1}{2} \left[(v^-_{j+\frac{1}{2}})^2 + (v^+_{j-\frac{1}{2}})^2 \right] \right\}^{\frac{1}{2}}.$$

For more detailed discussions on this issue, please see [15, 21].

3.1.2. Properties of the DG discretization. An application of integration by parts yields the next lemma, which plays an important role in the following analysis. See [2, 29] for details.

LEMMA 3.1. *The DG discretization has the following approximate skew-symmetric property:*

$$\mathcal{H}(w, v) + \mathcal{H}(v, w) = -2\beta(\theta - 1/2) \sum_{1 \leq j \leq J} [\![w]\!]_{j+\frac{1}{2}} [\![v]\!]_{j+\frac{1}{2}} \tag{3.3}$$

for any w and $v \in V_h$.

Remark 3.1. If the right-hand side of (3.3) is always equal to zero, this property is called the strictly skew-symmetric property. It happens when $\theta = 1/2$.

As a corollary, the DG discretization has the negative semidefinite property

$$\mathcal{H}(w, w) = -\beta(\theta - 1/2) \|[\![w]\!]\|^2_{\Gamma_h} \leq 0 \quad \forall\, w \in V_h, \tag{3.4}$$

which explicitly shows the stability contribution owing to the spatial discretization. Similar to the result in Sun and Shu [24, Lemma 2.3], the following development provides deeper insight into this issue. For the completeness of this paper, we give a simplified proof again.

LEMMA 3.2. *Let $\mathbb{G} = \{g_{ij}\}$ be a symmetric positive semidefinite matrix whose row numbers and column numbers are both taken from a given set $\mathcal{G}$. For any family $\{w_i\}_{i \in \mathcal{G}} \subset V_h$, there holds*

$$\sum_{i \in \mathcal{G}} \sum_{j \in \mathcal{G}} g_{ij} \mathcal{H}(w_i, w_j) \leq 0. \tag{3.5}$$

Proof. Consider the eigenvalue decomposition $\mathbb{G} = \mathbb{Q}^\top \mathrm{diag}(\sigma_i)\mathbb{Q}$, where $\mathbb{Q} = (q_{ij})$ is an orthonormal matrix, and $\mathrm{diag}(\sigma_i)$ is a diagonal matrix consisting of the nonnegative eigenvalues. Namely, there holds $g_{ij} = \sum_{\ell\in\mathcal{G}} q_{\ell i}\sigma_\ell q_{\ell j}$. This implies

$$\sum_{i\in\mathcal{G}}\sum_{j\in\mathcal{G}} g_{ij}\mathcal{H}(w_i, w_j) = \sum_{\ell\in\mathcal{G}} \sigma_\ell \mathcal{H}\left(\sum_{i\in\mathcal{G}} q_{\ell i} w_i, \sum_{j\in\mathcal{G}} q_{\ell j} w_j\right).$$

Since the arguments in the DG discretization are the same, we can complete the proof of this lemma by using (3.4). ∎

By applying the inverse properties and the Cauchy–Schwarz inequality, we easily obtain the following lemma, which will be used to determine the CFL condition.

LEMMA 3.3. *The DG discretization is continuous in $V_h \times V_h$ in the sense that*

$$|\mathcal{H}(w, v)| \le C|\beta|h^{-1}\|w\|\|v\| \quad \forall\, w, v \in V_h, \tag{3.6}$$

where the bounding constant $C > 0$ solely depends on θ and μ.

3.2. Temporal differences of stage solutions. For the stage solutions after the time level t^n, we would like to adopt the key concepts in [28, 29] and recursively define a series of the temporal differences in the form

$$\mathbb{D}_\kappa u^n = \sum_{0\le\ell\le\kappa} \sigma_{\kappa\ell} u^{n,\ell}, \quad \kappa \ge 1, \tag{3.7}$$

such that $\sum_{0\le\ell\le\kappa}\sigma_{\kappa\ell} = 0$ and

$$(\mathbb{D}_\kappa u^n, v) = \tau\mathcal{H}(\mathbb{D}_{\kappa-1}u^n, v) \quad \forall\, v \in V_h. \tag{3.8}$$

Here and below we denote $\mathbb{D}_0 u^n = u^n$ for simplicity. Owing to the relationship (3.8) and the definition of $\mathcal{H}(\cdot,\cdot)$, the temporal differences can be viewed as an approximation of certain time derivatives multiplying a constant depending on the time step.

LEMMA 3.4. *There exists a constant $C > 0$ solely depending on θ and μ, such that*

$$\|\mathbb{D}_\kappa u^n\| \le C\lambda\|\mathbb{D}_{\kappa-1}u^n\|, \quad \kappa \ge 1, \tag{3.9}$$

holds for any $n \ge 0$.

Proof. The proof is straightforward by taking $v = \mathbb{D}_\kappa u^n$ in (3.8) and employing Lemma 3.3. ∎

These temporal differences are very easily obtained by a linear combination of the schemes, since the spatial discretization is linear. Actually, this process does not depend on the particular definition of the spatial discretization, since the temporal differences solely depend on the fashion of time-marching.

3.3. Transferring of energy equations. In the above process to define the temporal differences, we also achieve the evolution identity

$$\alpha_0 u^{n+m} = \sum_{0\le i\le ms} \alpha_i \mathbb{D}_i u^n, \tag{3.10}$$

where $\alpha_0 > 0$ is used only for scaling. For convenience, denote $\boldsymbol{\alpha} = (\alpha_0, \alpha_1, \ldots, \alpha_{ms})$.

By taking the L^2-norm on both sides of (3.10), we have the energy equation

$$\alpha_0^2(\|u^{n+m}\|^2 - \|u^n\|^2) = \sum_{0\le i,j\le ms} a_{ij}(\mathbb{D}_i u^n, \mathbb{D}_j u^n) \equiv \mathrm{RHS}, \tag{3.11}$$

where $a_{00} = 0$ and $a_{ij} = \alpha_i\alpha_j$ if $i + j > 0$. This expression is not very useful for the stability analysis since the stability contribution of the particular spatial discretization is not reflected. Hence we introduce a simple transferring to write the right-hand side of (3.11) into an equivalent but more useful expression, which is denoted in the form

$$\mathrm{RHS}(\ell) = \sum_{0\le i,j\le ms} a_{ij}^{(\ell)}(\mathbb{D}_i u^n, \mathbb{D}_j u^n) + \sum_{0\le i,j\le ms} b_{ij}^{(\ell)}\tau\mathcal{H}(\mathbb{D}_i u^n, \mathbb{D}_j u^n). \tag{3.12}$$

For notational convenience, we express (3.12) by two symmetric matrices of $(ms+1)$th order,

$$\mathbb{A}^{(\ell)} = \{a_{ij}^{(\ell)}\}, \quad \mathbb{B}^{(\ell)} = \{b_{ij}^{(\ell)}\}, \tag{3.13}$$

where the row number i and column number j are both taken from $\{0, 1, \ldots, ms\}$. Obviously, the matrices $\mathbb{A}^{(0)} = \{a_{ij}\}$ and $\mathbb{B}^{(0)} = \mathbb{O}$ are given, for the initial situation.

The motivation of matrix transferring in (3.12) is due to two issues. One is the relationship (3.8) among those temporal differences. The other is the full usage of the approximate skew-symmetric property of the spatial discretization, which has been stated in Lemma 3.1.

Below we present the detailed implementation. Assume that the ℓth transferring starts from the given matrix

$$\mathbb{A}^{(\ell)} = \left[\begin{array}{c|c|ccc} \mathbb{O} & \mathbb{O} & \mathbb{O} & \cdots & \mathbb{O} \\ \hline \mathbb{O} & a_{\ell\ell}^{(\ell)} & a_{\ell,\ell+1}^{(\ell)} & \cdots & a_{\ell,ms}^{(\ell)} \\ \hline \mathbb{O} & a_{\ell+1,\ell}^{(\ell)} & a_{\ell+1,\ell+1}^{(\ell)} & \cdots & a_{\ell+1,ms}^{(\ell)} \\ \vdots & \vdots & \vdots & \ddots & \vdots \\ \mathbb{O} & a_{ms,\ell}^{(\ell)} & a_{ms,\ell+1}^{(\ell)} & \cdots & a_{ms,ms}^{(\ell)} \end{array}\right]. \tag{3.14}$$

Note that those zeros at the left and the top do not exist if $\ell = 0$ since $\mathbb{A}^{(0)} = \{a_{ij}\}$.

If $a_{\ell\ell}^{(\ell)} \neq 0$, then the transferring process stops, and the *termination index* is defined as $\zeta = \ell$. For the initial situation, $a_{00}^{(0)} = a_{00} = 0$; hence $1 \le \zeta \le ms$.

Otherwise, if $a_{\ell\ell}^{(\ell)} = 0$, the following transferring process will be carried out to get new matrices $\mathbb{A}^{(\ell+1)}$ and $\mathbb{B}^{(\ell+1)}$. The main action is to move the same-order temporal information into an equivalent expression of spatial information. Here the temporal information refers to $(\mathbb{D}_i u^n, \mathbb{D}_j u^n)$, whose coefficients are shown by the nonzero entries at the ℓth row (and column) of $\mathbb{A}^{(\ell)}$. The spatial information refers to $\tau\mathcal{H}(\mathbb{D}_i u^n, \mathbb{D}_j u^n)$, whose coefficients are shown by the entries at the ℓth row (and column) of $\mathbb{B}^{(\ell+1)}$. By making full use of the relationship (3.8) among those temporal differences, we have

$$2a_{\ell+1,\ell}^{(\ell)}(\mathbb{D}_{\ell+1}u^n, \mathbb{D}_\ell u^n) = 2a_{\ell+1,\ell}^{(\ell)}\Big[\tau\mathcal{H}(\mathbb{D}_\ell u^n, \mathbb{D}_\ell u^n)\Big], \tag{3.15a}$$

and for $\ell + 1 \le i \le ms - 1$,

(3.15b)

$$\begin{aligned} &2a_{i+1,\ell}^{(\ell)}(\mathbb{D}_{i+1}u^n, \mathbb{D}_\ell u^n) + Q_{i,\ell+1}a_{i,\ell+1}^{(\ell)}(\mathbb{D}_i u^n, \mathbb{D}_{\ell+1}u^n) \\ &= Q_{i,\ell+1}\Big[a_{i,\ell+1}^{(\ell)} - \frac{2a_{i+1,\ell}^{(\ell)}}{Q_{i,\ell+1}}\Big](\mathbb{D}_i u^n, \mathbb{D}_{\ell+1}u^n) + 2a_{i+1,\ell}^{(\ell)}\Big[\tau\mathcal{H}(\mathbb{D}_i u^n, \mathbb{D}_\ell u^n) + \tau\mathcal{H}(\mathbb{D}_\ell u^n, \mathbb{D}_i u^n)\Big]. \end{aligned}$$

Here $Q_{i,\ell+1}$ is equal to 1 if $i = \ell + 1$, or equal to 2 otherwise. Writing the above coefficients in the matrices $\mathbb{A}^{(\ell+1)}$ and $\mathbb{B}^{(\ell+1)}$, we can define the transferring as follows:

$$a_{ij}^{(\ell+1)} = \begin{cases} 0, & 0 \le j \le \ell, \\ a_{ij}^{(\ell)} - 2a_{i+1,j-1}^{(\ell)}, & i = \ell+1 \text{ and } j = \ell+1, \\ a_{ij}^{(\ell)} - a_{i+1,j-1}^{(\ell)}, & \ell+2 \le i \le ms-1 \text{ and } j = \ell+1, \\ a_{ij}^{(\ell)} & \text{otherwise}, \end{cases} \tag{3.16}$$

and

$$b_{ij}^{(\ell+1)} = \begin{cases} 2a_{i+1,j}^{(\ell)}, & \ell \le i \le ms-1 \text{ and } j = \ell, \\ b_{ij}^{(\ell)} & \text{otherwise}. \end{cases} \tag{3.17}$$

Since the symmetric property is preserved in the transferring process, the above formulations are only given for the lower-triangular part of the matrices.

Remark 3.2. Following (3.16) and (3.17), we can see that the nonzero entries of $\mathbb{A}^{(\ell)}$ and the zero entries of $\mathbb{B}^{(\ell)}$ are mainly located at the right and the bottom. In each matrix transferring, only two rows (and columns) are different between $\mathbb{A}^{(\ell)}$ and $\mathbb{A}^{(\ell+1)}$, and only one row (and column) is different between $\mathbb{B}^{(\ell)}$ and $\mathbb{B}^{(\ell+1)}$.

3.4. Discussions and statements. Below we use $\mathcal{Q}_1(\lambda)$ and $\mathcal{Q}_2(\lambda)$ to denote generic polynomials of the CFL number λ with nonnegative coefficients. They are always bounded if the CFL number is smaller than 1. Their expression may be different at each occurrence.

In what follows we separately estimate two terms in RHS(ζ), where ζ is the termination index. The first term solely includes the inner product of the temporal differences. By using Lemma 3.4 and the Cauchy–Schwarz inequality, we have

$$\sum_{0 \le i,j \le ms} a_{ij}^{(\zeta)} (\mathbb{D}_i u^n, \mathbb{D}_j u^n) \le \left[a_{\zeta\zeta}^{(\zeta)} + \lambda \mathcal{Q}_1(\lambda) \right] \|\mathbb{D}_\zeta u^n\|^2, \tag{3.18}$$

where λ is the CFL number, and $a_{\zeta\zeta}^{(\zeta)} \neq 0$.

The second term in RHS(ζ) explicitly shows the detailed contribution of the spatial discretization. Associated with the matrix $\mathbb{B}^{(\zeta)}$, we define the index set of the bad submatrices

$$\mathcal{B} = \{\kappa \colon \det \mathbb{B}_\kappa^{(\zeta)} \le 0, \text{ and } 0 \le \kappa \le \zeta - 1\}, \tag{3.19}$$

where $\mathbb{B}_\kappa^{(\zeta)} = \{b_{ij}^{(\zeta)}\}_{0 \le i,j \le \kappa}$ is the $(\kappa+1)$th order leading principal submatrix of $\mathbb{B}^{(\zeta)}$. Note that the lower-order leading principal submatrix is preserved at the subsequent transferring process, which implies $\mathbb{B}_\kappa^{(\zeta)} = \mathbb{B}_\kappa^{(\kappa+1)}$, and that the index set $\mathcal{B}$ can be obtained along the transferring process. Then we define the *contribution index* of the spatial discretization as

$$\rho = \begin{cases} \min\{i : i \in \mathcal{B}\} & \text{if } \mathcal{B} \neq \emptyset, \\ \zeta & \text{otherwise}. \end{cases} \tag{3.20}$$

It follows from the definition that $0 \le \rho \le \zeta$. Define three sets

$$\pi_1 = \{0, 1, \ldots, \rho - 1\}, \quad \pi_2 = \{\rho, \rho+1, \ldots, \zeta - 1\}, \quad \pi_3 = \{\zeta, \zeta+1, \ldots, ms\}. \tag{3.21}$$

They form a partition of $\{0, 1, \ldots, ms\}$. Note that $\pi_1 = \emptyset$ if $\rho = 0$, and $\pi_2 = \emptyset$ if $\rho = \zeta$. In the following, we are going to estimate each term in the separation

$$\sum_{0\le i,j\le ms} \tau b_{ij}^{(\zeta)} \mathcal{H}(\mathbb{D}_i u^n, \mathbb{D}_j u^n) = \sum_{\xi,\eta=1,2,3} T_{\xi\eta}, \tag{3.22}$$

where the row numbers and column numbers in each term are taken from one of the three subsets, namely

$$T_{\xi\eta} = \sum_{i\in\pi_\xi, j\in\pi_\eta} \tau b_{ij}^{(\zeta)} \mathcal{H}(\mathbb{D}_i u^n, \mathbb{D}_j u^n). \tag{3.23}$$

If one set is empty, the corresponding terms are equal to zero.

As a result of the definition (3.20), the submatrix $\mathbb{B}_{\rho-1}^{(\zeta)}$ is positive definite. Hence, there exists a constant $\varepsilon > 0$, for example, the smallest eigenvalue, such that $\mathbb{B}_{\rho-1}^{(\zeta)} - \varepsilon\mathbb{I}_{\rho-1}$ is positive semidefinite, where $\mathbb{I}_{\rho-1}$ is the identity matrix. Owing to Lemma 3.2 and identity (3.4), we have

$$T_{11} \le -\varepsilon\beta\left(\theta - \frac{1}{2}\right)\tau \sum_{i\in\pi_1} \|[\![\mathbb{D}_i u^n]\!]\|_{\Gamma_h}^2. \tag{3.24}$$

Owing to the approximate skew-symmetric property (Lemma 3.1), Young's inequality, the second inverse inequality, and the relationship among temporal differences (Lemma 3.4), we have

(3.25)

$$\begin{aligned} T_{12} + T_{21} =& -\beta\left(\theta - \frac{1}{2}\right)\tau \sum_{i\in\pi_1, j\in\pi_2} b_{ij}^{(\zeta)} \|[\![\mathbb{D}_i u^n]\!]\|_{\Gamma_h} \|[\![\mathbb{D}_j u^n]\!]\|_{\Gamma_h} \\ \le& \frac{1}{4}\varepsilon\beta\left(\theta - \frac{1}{2}\right)\tau \sum_{i\in\pi_1} \|[\![\mathbb{D}_i u^n]\!]\|_{\Gamma_h}^2 + \varepsilon^{-1}\beta\left(\theta - \frac{1}{2}\right)(\zeta - \rho)\tau \sum_{j\in\pi_2} \Big[\sum_{i\in\pi_1} (b_{ij}^{(\zeta)})^2\Big] \|[\![\mathbb{D}_j u^n]\!]\|_{\Gamma_h}^2 \\ \le& \frac{1}{4}\varepsilon\beta\left(\theta - \frac{1}{2}\right)\tau \sum_{i\in\pi_1} \|[\![\mathbb{D}_i u^n]\!]\|_{\Gamma_h}^2 + \lambda\mathcal{Q}_2(\lambda)\|\mathbb{D}_\rho u^n\|^2. \end{aligned}$$

Similarly, we also have

$$T_{22} + T_{23} + T_{32} \le \lambda\mathcal{Q}_2(\lambda)\|\mathbb{D}_\rho u^n\|^2 + \lambda\mathcal{Q}_2(\lambda)\|\mathbb{D}_\zeta u^n\|^2. \tag{3.26}$$

Along the same lines, we have

$$T_{13} + T_{31} \le \frac{1}{4}\varepsilon\beta\left(\theta - \frac{1}{2}\right)\tau \sum_{i\in\pi_1} \|[\![\mathbb{D}_i u^n]\!]\|_{\Gamma_h}^2 + \lambda\mathcal{Q}_1(\lambda)\|\mathbb{D}_\zeta u^n\|^2. \tag{3.27}$$

Furthermore, it is trivial to see that $T_{33} = 0$, since all related coefficients are zero. Collecting the above estimations, we have the inequality

$$\alpha_0^2(\|u^{n+m}\|^2 - \|u^n\|^2) \le \mathcal{Y}_1 + \mathcal{Y}_2, \tag{3.28}$$

where different stability mechanisms are shown in

$$\mathcal{Y}_1 = \Big[a_{\zeta\zeta}^{(\zeta)} + \lambda\mathcal{Q}_1(\lambda) + \lambda\mathcal{Q}_2(\lambda)\Big]\|\mathbb{D}_\zeta u^n\|^2 + \lambda\mathcal{Q}_2(\lambda)\|\mathbb{D}_\rho u^n\|^2, \tag{3.29a}$$

$$\mathcal{Y}_2 = -\frac{1}{2}\varepsilon\beta\left(\theta - \frac{1}{2}\right)\tau \sum_{0\le i\le\rho-1} \|[\![\mathbb{D}_i u^n]\!]\|_{\Gamma_h}^2. \tag{3.29b}$$

In the first term $\mathcal{Y}_1$, the polynomials $\mathcal{Q}_1(\cdot)$ and $\mathcal{Q}_2(\cdot)$ show the negative effects due to the time-marching, and the approximate skew-symmetric property of the spatial DG discretization, respectively. The second term $\mathcal{Y}_2$, which is always nonpositive, shows the good stability mechanism inherited from the spatial DG discretization.

We are now ready to present the main theorem in this paper, where the second stability mechanism is omitted. The sign of $a_{\zeta\zeta}^{(\zeta)} \neq 0$ strongly affects the stability conclusion of the RKDG schemes.

THEOREM 3.1. *Let $m = 1$. With the termination index ζ and the contribution index ρ obtained by the above matrix transferring process, we have the following statements for the RKDG scheme.*

1. *If $a_{\zeta\zeta}^{(\zeta)} < 0$ and $\rho = \zeta$, then the scheme has monotonicity stability.*
2. *If $a_{\zeta\zeta}^{(\zeta)} < 0$ and $\rho < \zeta$, then the scheme has weak$(2\rho + 1)$ stability.*
3. *If $a_{\zeta\zeta}^{(\zeta)} > 0$, then the scheme has weak(γ) stability with $\gamma = \min(2\zeta, 2\rho + 1)$.*

Proof. Since $a_{\zeta\zeta}^{(\zeta)} < 0$ and $\rho = \zeta$, we can get

$$\mathcal{Y}_1 = \left[a_{\zeta\zeta}^{(\zeta)} + \lambda\mathcal{Q}_1(\lambda) + \lambda\mathcal{Q}_2(\lambda)\right]\|\mathbb{D}_\zeta u^n\|^2 \leq 0$$

if the CFL number λ is small enough. This implies the first conclusion.

If $a_{\zeta\zeta}^{(\zeta)} < 0$ and $\rho < \zeta$, we can still keep the nonpositivity as above if the CFL number is small enough. As a result, we can get from Lemma 3.4 that

$$\mathcal{Y}_1 \leq C\lambda\|\mathbb{D}_\rho u^n\|^2 \leq C\lambda^{2\rho+1}\|u^n\|^2,$$

which implies the second conclusion.

The last conclusion can be obtained along the same lines, so the proof is omitted. ∎

The second stability mechanism will be discussed in more depth in section 5. If this mechanism is not equal to zero, it may help us to obtain the monotonicity stability for some of the lower-degree polynomials, like the RKDG(2,2,1) method in [28].

Before we discuss examples of the RKDG methods in the next section, we would like to give an explanation of the conclusion of Theorem 3.1.

- The first conclusion focuses on the case that neither the temporal nor the spatial discretization produces any antidissipative energy. Hence, the monotonicity stability holds in this case. An example is the RKDG$(3, 3, k)$ method in section 4.3.
- The second conclusion points to an intermediate state that the temporal discretization provides dissipative energy, but the spatial discretization causes some antidissipative modes that must be controlled by reducing the time step. This trouble results from the approximate skew-symmetric property in $\mathcal{H}(\cdot, \cdot)$. More discussions are given in the next remark.
- The third conclusion focuses on the case that the temporal discretization has an antidissipative energy that can only be controlled through a time-step reduction. Two well-known examples are the RKDG$(1, 1, k)$ method and the RKDG$(2, 2, k)$ method; see sections 4.1 and 4.2, respectively.

Remark 3.3. It is worth mentioning that the second conclusion in Theorem 3.1 is not good enough to show the real performance of stability. This weak conclusion is achieved by the approximate skew-symmetric property of the spatial discretization and the statement for one-step time-marching. Two comments are given here.

- If the functions in V_h are restricted to being continuous (the DG method degenerates to the standard finite element method) or the central numerical flux (i.e., $\theta = 1/2$) is used, there holds the strictly skew-symmetric property for $\mathcal{H}(\cdot,\cdot)$, which leads to $\mathcal{Q}_2(\cdot) = 0$. Along the same lines as the previous analysis, we can prove that the fully discrete scheme has monotonicity stability since the spatial discretization does not cause any trouble in the L^2-norm stability for the semidiscrete scheme.
- For many schemes related to this conclusion (at least those considered in this paper), we often get $\rho = \zeta - 1$ for one-step time-marching. In this case, we have a great opportunity to establish the monotonicity stability of multiple-step time-marching, which together with the second conclusion in Theorem 3.1 derives the strong stability. See the RKDG$(4,4,k)$ scheme in section 4.4 as an example.

To conclude this section, we would like to point out that the technique used in Theorem 3.1 can be applied in the stability analysis for many fully discrete methods. The key point in this analysis is the interplay between the stability mechanism of the temporal discretization and the dissipative effect of the spatial discretization, which is easily implemented with the help of temporal differences. More discussion about this issue will be given in section 5, when the lower polynomial degree is used in the RKDG methods.

4. RKDG methods with the same stages and order. In this section we show the flexibility and effectiveness of the above framework and present the detailed proof of Theorem 2.1 for $r \le 4$. The proofs for the other schemes are similar; hence they are omitted for brevity.

4.1. First order scheme. Let us start with Euler-forward time-marching, which is implemented as follows. For any test function $v \in V_h$, the following variational formula holds:

$$(u^{n+1}, v) = (u^n, v) + \tau \mathcal{H}(u^n, v). \tag{4.1}$$

The stability result is stated in the following proposition.

PROPOSITION 4.1. *The RKDG$(1,1,k)$ scheme has weak(2) stability.*

Proof. It is easy to see that $\mathbb{D}_1 u^n = u^{n+1} - u^n$, which implies $\boldsymbol{\alpha} = (1,1)$ and

$$\mathbb{A}^{(0)} = \begin{bmatrix} 0 & 1 \\ 1 & 1 \end{bmatrix}, \quad \mathbb{B}^{(0)} = \mathbb{O}. \tag{4.2}$$

Since $a_{00}^{(0)} = 0$, we transform the energy equation into an equivalent form with

$$\mathbb{A}^{(1)} = \left[\begin{array}{c:c} 0 & \\ \hdashline & 1 \end{array}\right], \quad \mathbb{B}^{(1)} = \left[\begin{array}{c:c} 2 & 0 \\ \hdashline 0 & 0 \end{array}\right]. \tag{4.3}$$

Since $a_{11}^{(1)} = 1 > 0$, we stop the transferring. It is easy to see that $\rho = \zeta = 1$, which implies weak(2) stability. ∎

4.2. Second order scheme. The RKDG$(2,2,k)$ scheme is implemented as follows. For any test function $v \in V_h$, the following variational formulas hold:

$$(u^{n,1}, v) = (u^n, v) + \tau \mathcal{H}(u^n, v), \tag{4.4a}$$

$$(u^{n+1}, v) = \frac{1}{2}(u^n, v) + \frac{1}{2}(u^{n,1}, v) + \frac{\tau}{2}\mathcal{H}(u^{n,1}, v). \tag{4.4b}$$

The stability result is stated in the following proposition.

PROPOSITION 4.2. *The RKDG(2, 2, k) scheme has weak(4) stability.*

Proof. By the first equation of this scheme, we have $u^{n,1} = u^n + \mathbb{D}_1 u^n$. Putting it into the second equation, we have

$$\begin{aligned}(u^{n+1}, v) &= \frac{1}{2}(\mathbb{D}_0 u^n, v) + \frac{1}{2}(\mathbb{D}_0 u^n + \mathbb{D}_1 u^n, v) + \frac{\tau}{2}\mathcal{H}(\mathbb{D}_0 u^n + \mathbb{D}_1 u^n, v)\\ &= \frac{1}{2}(\mathbb{D}_0 u^n, v) + \frac{1}{2}(\mathbb{D}_0 u^n + \mathbb{D}_1 u^n, v) + \frac{1}{2}(\mathbb{D}_1 u^n + \mathbb{D}_2 u^n, v)\\ &= (\mathbb{D}_0 u^n + \mathbb{D}_1 u^n + \frac{1}{2}\mathbb{D}_2 u^n, v)\end{aligned}$$

for any test function $v \in V_h$. Hence we have the evolution identity

$$2u^{n+1} = 2\mathbb{D}_0 u^n + 2\mathbb{D}_1 u^n + \mathbb{D}_2 u^n, \tag{4.5}$$

with $\boldsymbol{\alpha} = (2, 2, 1)$ and the temporal differences

$$\begin{bmatrix}\mathbb{D}_0 u^n\\ \mathbb{D}_1 u^n\\ \mathbb{D}_2 u^n\end{bmatrix} = \begin{bmatrix}1 & & \\ -1 & 1 & \\ 0 & -2 & 2\end{bmatrix}\begin{bmatrix}u^n\\ u^{n,1}\\ u^{n+1}\end{bmatrix}. \tag{4.6}$$

As we have shown in the previous section, the initial energy equation can be expressed by the matrices

$$\mathbb{A}^{(0)} = \begin{bmatrix}0 & 4 & 2\\ 4 & 4 & 2\\ 2 & 2 & 1\end{bmatrix}, \quad \mathbb{B}^{(0)} = \mathbb{O}. \tag{4.7}$$

Since $a_{00}^{(0)} = 0$, we need to carry out the transferring and get that

$$\mathbb{A}^{(1)} = \left[\begin{array}{c|cc} 0 & & \\ \hline & 0 & 2\\ & 2 & 1\end{array}\right], \quad \mathbb{B}^{(1)} = \left[\begin{array}{c|cc} 8 & 4 & 0\\ \hline 4 & 0 & 0\\ 0 & 0 & 0\end{array}\right]. \tag{4.8}$$

Since $a_{11}^{(1)} = 0$, we continue the transferring process and get

$$\mathbb{A}^{(2)} = \left[\begin{array}{cc|c} 0 & & \\ & 0 & \\ \hline & & 1\end{array}\right], \quad \mathbb{B}^{(2)} = \left[\begin{array}{cc|c} 8 & 4 & 0\\ 4 & 4 & 0\\ \hline 0 & 0 & 0\end{array}\right]. \tag{4.9}$$

Since $a_{22}^{(2)} = 1 > 0$, we stop the transferring and get $\zeta = 2$. Also, it is easy to see that $\rho = 2$. Then it follows from Lemma 3.1 that the scheme has weak(4) stability. ∎

Remark 4.1. A similar weak L^2-norm stability result has been implicitly given in [28] that a stronger condition $\tau = \mathcal{O}(h^{4/3})$ is needed for the stability with higher-order ($k \geq 2$) piecewise polynomials.

4.3. Third order scheme. The RKDG(3, 3, k) scheme is implemented as follows. For any test function $v \in V_h$, the following variational formulas hold:

$$(u^{n,\ell+1}, v) = (u^{n,\ell}, v) + \tau\mathcal{H}(u^{n,\ell}, v), \qquad \ell = 0, 1, \tag{4.10a}$$

$$(u^{n+1}, v) = \frac{1}{3}(u^n, v) + \frac{1}{2}(u^{n,1}, v) + \frac{1}{6}(u^{n,2}, v) + \frac{\tau}{6}\mathcal{H}(u^{n,2}, v). \tag{4.10b}$$

The stability result is shown in the following proposition, which is the same as that in [29].

PROPOSITION 4.3. *The RKDG(3, 3, k) scheme has monotonicity stability.*

Proof. By some linear combinations of the RKDG(3, 3, k) scheme, it is easy to define the temporal differences in the form

$$\begin{bmatrix} \mathbb{D}_0 u^n \\ \mathbb{D}_1 u^n \\ \mathbb{D}_2 u^n \\ \mathbb{D}_3 u^n \end{bmatrix} = \begin{bmatrix} 1 & & & \\ -1 & 1 & & \\ 1 & -2 & 1 & \\ -3 & 0 & -3 & 6 \end{bmatrix} \begin{bmatrix} u^n \\ u^{n,1} \\ u^{n,2} \\ u^{n+1} \end{bmatrix} \tag{4.11}$$

and get the evolution identity

$$6u^{n+1} = 6\mathbb{D}_0 u^n + 6\mathbb{D}_1 u^n + 3\mathbb{D}_2 u^n + \mathbb{D}_3 u^n. \tag{4.12}$$

This implies $\boldsymbol{\alpha} = (6, 6, 3, 1)$ and the initial matrices

$$\mathbb{A}^{(0)} = \begin{bmatrix} 0 & 36 & 18 & 6 \\ 36 & 36 & 18 & 6 \\ 18 & 18 & 9 & 3 \\ 6 & 6 & 3 & 1 \end{bmatrix}, \quad \mathbb{B}^{(0)} = \mathbb{O}. \tag{4.13}$$

The first transferring leads to

$$\mathbb{A}^{(1)} = \left[\begin{array}{c|ccc} 0 & & & \\ \hline & 0 & 12 & 6 \\ & 12 & 9 & 3 \\ & 6 & 3 & 1 \end{array}\right], \quad \mathbb{B}^{(1)} = \left[\begin{array}{c|ccc} 72 & 36 & 12 & 0 \\ \hline 36 & 0 & 0 & 0 \\ 12 & 0 & 0 & 0 \\ 0 & 0 & 0 & 0 \end{array}\right]. \tag{4.14}$$

The second transferring leads to

$$\mathbb{A}^{(2)} = \left[\begin{array}{cc|cc} 0 & & & \\ & 0 & & \\ \hline & & -3 & 3 \\ & & 3 & 1 \end{array}\right], \quad \mathbb{B}^{(2)} = \left[\begin{array}{cc|cc} 72 & 36 & 12 & 0 \\ 36 & 24 & 12 & 0 \\ \hline 12 & 12 & 0 & 0 \\ 0 & 0 & 0 & 0 \end{array}\right]. \tag{4.15}$$

Since $a_{22}^{(2)} = -3 < 0$, the transferring process is terminated with $\zeta = 2$. Furthermore, it is easy to see $\rho = 2$, since the two leading principal determinants are respectively equal to 72 and 432. By applying Lemma 3.1, we complete the proof of this proposition. ∎

Remark 4.2. In the above analysis, it is very important that the term $-3\|\mathbb{D}_2 u^n\|^2$ provides an additional stability mechanism (or dissipative energy) owing to the time-discretization. This result is the same as that in [21, 29]. In this paper we give a new and simpler analysis process based on matrix transferring, which is more natural and easier to systematically extend to higher-order time-marching.

4.4. Fourth order scheme. Let us consider the RKDG(4, 4, k) scheme, where the coefficients are defined by Table 1. For any test function $v \in V_h$, the following variational formulas hold:

$$(u^{n,\ell+1}, v) = (u^{n,\ell}, v) + \tau \mathcal{H}(u^{n,\ell}, v), \qquad \ell = 0, 1, 2, \tag{4.16a}$$

$$(u^{n+1}, v) = \frac{3}{8}(u^n, v) + \frac{1}{3}(u^{n,1}, v) + \frac{1}{4}(u^{n,2}, v) + \frac{1}{24}(u^{n,3}, v) + \frac{1}{24}\tau \mathcal{H}(u^{n,3}, v). \tag{4.16b}$$

The stability result is shown in the following proposition, which is similar to and slightly stronger than the result in [24].

PROPOSITION 4.4. *The RKDG(4, 4, k) scheme has strong stability for* $n \geq 2$.

Proof. First consider one-step time-marching. By induction, we can define the temporal differences in the form

$$\begin{bmatrix} \mathbb{D}_0 u^n \\ \mathbb{D}_1 u^n \\ \mathbb{D}_2 u^n \\ \mathbb{D}_3 u^n \\ \mathbb{D}_4 u^n \end{bmatrix} = \begin{bmatrix} 1 & & & & \\ -1 & 1 & & & \\ 1 & -2 & 1 & & \\ -1 & 3 & -3 & 1 & \\ -8 & -12 & 0 & -4 & 24 \end{bmatrix} \begin{bmatrix} u^n \\ u^{n,1} \\ u^{n,2} \\ u^{n,3} \\ u^{n+1} \end{bmatrix} \tag{4.17}$$

and obtain the evolution identity

$$24u^{n+1} = 24\mathbb{D}_0 u^n + 24\mathbb{D}_1 u^n + 12\mathbb{D}_2 u^n + 4\mathbb{D}_3 u^n + \mathbb{D}_4 u^n, \tag{4.18}$$

with $\boldsymbol{\alpha} = (24, 24, 12, 4, 1)$. For the sake of brevity, we present only the final matrices in the energy equation:

$$\mathbb{A}^{(3)} = \left[\begin{array}{ccc:cc} 0 & & & & \\ & 0 & & & \\ & & 0 & & \\ \hdashline & & & -8 & 4 \\ & & & 4 & 1 \end{array}\right], \quad \mathbb{B}^{(3)} = \left[\begin{array}{ccc:cc} 1152 & 576 & 192 & 48 & 0 \\ 576 & 384 & 144 & 48 & 0 \\ 192 & 144 & 48 & 24 & 0 \\ \hdashline 48 & 48 & 24 & 0 & 0 \\ 0 & 0 & 0 & 0 & 0 \end{array}\right]. \tag{4.19}$$

Namely, the termination index is $\zeta = 3$, and $a_{33}^{(3)} = -8 < 0$. It is easy to see $\rho = 2 = \zeta - 1$, since the three leading principal minors in order are $1152, 110592$, and -884736. As a result of Lemma 3.1, the RKDG$(4, 4, k)$ scheme with one-step time-marching is of weak(5) stability.

To prove this proposition, we need to show the monotonicity stability for combining multiple time steps in the time-marching.

Updating the solution from t^n to t^{n+2} by using the RKDG$(4, 4, k)$ method for two consecutive time steps is looked upon as a one-step time-marching by the RKDG$(8, 4, k)$ method. In addition to (4.17), four more temporal differences are recursively defined in the form

$$\begin{bmatrix} \mathbb{D}_5 u^n \\ \mathbb{D}_6 u^n \\ \mathbb{D}_7 u^n \\ \mathbb{D}_8 u^n \end{bmatrix} = \begin{bmatrix} 44 & 36 & 12 & 4 & -120 & 24 & & & \\ -80 & -24 & 0 & 8 & 216 & -144 & 24 & & \\ 8 & -120 & -72 & -8 & -24 & 360 & -168 & 24 & \\ 64 & 192 & 0 & -64 & -384 & -576 & 384 & -192 & 576 \end{bmatrix} \mathbf{u}^n, \tag{4.20}$$

where $\mathbf{u}^n = (u^n, u^{n,1}, u^{n,2}, \ldots, u^{n,6}, u^{n,7}, u^{n+2})^\top$, and we then obtain the evolution identity

$$\alpha_0 u^{n+2} = \sum_{0 \leq i \leq 8} \alpha_i \mathbb{D}_i u^n, \tag{4.21}$$

with $\boldsymbol{\alpha} = (576, 1152, 1152, 768, 384, 144, 40, 8, 1)$. After three transferring processes,

we obtain

$$\mathbb{A}^{(3)} = \left[\begin{array}{ccc:cccccc} 0 & & & & & & & & \\ & 0 & & & & & & & \\ & & 0 & & & & & & \\ \hdashline & & & -9216 & 170496 & 73152 & 22656 & 4992 & 768 \\ & & & 170496 & 147456 & 55296 & 15360 & 3072 & 384 \\ & & & 73152 & 55296 & 20736 & 5760 & 1152 & 144 \\ & & & 22656 & 15360 & 5760 & 1600 & 320 & 40 \\ & & & 4992 & 3072 & 1152 & 320 & 64 & 8 \\ & & & 768 & 384 & 144 & 40 & 8 & 1 \end{array}\right]$$

and

$$\mathbb{B}^{(3)} = \left[\begin{array}{ccc:cccccc} 1327104 & 1327104 & 884736 & 442368 & 165888 & 46080 & 9216 & 1152 & 0 \\ 1327104 & 1769472 & 1327104 & 718848 & 285696 & 82944 & 17280 & 2304 & 0 \\ 884736 & 1327104 & 1050624 & 599040 & 248832 & 74880 & 16128 & 2304 & 0 \\ \hdashline 442368 & 718848 & 599040 & 0 & 0 & 0 & 0 & 0 & 0 \\ 165888 & 285696 & 248832 & 0 & 0 & 0 & 0 & 0 & 0 \\ 46080 & 82944 & 74880 & 0 & 0 & 0 & 0 & 0 & 0 \\ 9216 & 17280 & 16128 & 0 & 0 & 0 & 0 & 0 & 0 \\ 1152 & 2304 & 2304 & 0 & 0 & 0 & 0 & 0 & 0 \\ 0 & 0 & 0 & 0 & 0 & 0 & 0 & 0 & 0 \end{array}\right].$$

Since $a_{33}^{(3)} = -9216 < 0$, we stop the transferring process and get $\zeta = 3$. It is easy to see $\rho = 3$, since the three leading principal minors in order are $1327104, 587068342272$, and 10820843684757504. It follows from Lemma 3.1 that monotonicity stability is proved for combining two steps in the time-marching.

Updating the solution from t^n to t^{n+3} by combining three time steps of the RKDG$(4, 4, k)$ method is looked upon as a one-step time-marching by an RKDG$(12, 4, k)$ method. The analysis follows the same lines as before, but the process is more lengthy. We omit the intermediate steps of the detailed definitions of temporal differences up to the 12th order. Finally, we have the evolution identity (3.10) with

(4.22)
$$\boldsymbol{\alpha} = (13824, 41472, 62208, 62208, 46656, 27648, 13248, 5184, 1656, 424, 84, 12, 1).$$

The matrices $\mathbb{A}^{(3)}$ and $\mathbb{B}^{(3)}$ are shown in Tables 2 and 3, respectively. They show that the termination index is $\zeta = 3$, and $a_{33}^{(3)} = -7962624 < 0$. Also, it is easy to see that $\rho = 3$ since the three leading principal minors in order are $1146617856, 986049380773527552$, and $11777310696798643575324672 0$. Then it follows from Lemma 3.1 that the monotonicity stability is proved for three steps in the time-marching.

Starting from $n = 0$, the above two sequences cover all integers $n \geq 2$. By the above results for combining multiple time steps with both $m = 2$ and $m = 3$, we can conclude the strong stability for $n \geq 2$ and hence complete the proof of this proposition. ∎

Remark 4.3. The above performance of the RKDG$(4, 4, k)$ method shows the negative effect of the approximate skew-symmetric property of the spatial discretization. Although the jumps provide extra L^2-norm stability in the semidiscrete method, they might have a negative effect in the fully discrete method as the spatial operator is no

TABLE 2
The matrix $\mathbb{A}^{(3)}$: RKDG$(4,4,k)$ scheme and $m=3$.

0											
	0										
		0									
			-7962624	1660207104	1087893504	564461568	235892736	79958016	21634560	4520448	684288	62208
			1660207104	2176782336	1289945088	618098688	241864704	77262336	19782144	3919104	559872	46656
			1087893504	1289945088	764411904	366280704	143327232	45785088	11722752	2322432	331776	27648
			564461568	618098688	366280704	175509504	68677632	21938688	5617152	1112832	158976	13248
			235892736	241864704	143327232	68677632	26873856	8584704	2198016	435456	62208	5184
			79958016	77262336	45785088	21938688	8584704	2742336	702144	139104	19872	1656
			21634560	19782144	11722752	5617152	2198016	702144	179776	35616	5088	424
			4520448	3919104	2322432	1112832	435456	139104	35616	7056	1008	84
			684288	559872	331776	158976	62208	19872	5088	1008	144	12
			62208	46656	27648	13248	5184	1656	424	84	12	1

TABLE 3
The matrix $\mathbb{B}^{(3)}$: RKDG$(4,4,k)$ scheme and $m=3$.

1146617856	1719926784	1719926784	1289945088	764411904	366280704	143327232	45785088	11722752	2322432	331776	27648	0
1719926784	3439853568	3869835264	3105423360	1926955008	955514880	384196608	125632512	32845824	6635520	967680	82944	0
1719926784	3869835264	4634247168	3877797888	2484338688	1264066560	519340032	173187072	46116864	9483264	1410048	124416	0
1289945088	3105423360	3877797888	0									
764411904	1926955008	2484338688		0								
366280704	955514880	1264066560			0							
143327232	384196608	519340032				0						
45785088	125632512	173187072					0					
11722752	32845824	46116864						0				
2322432	6635520	9483264							0			
331776	967680	1410048								0		
27648	82944	124416									0	
0	0	0										0

longer normal. However, owing to $a^{(\zeta)}_{\zeta\zeta} < 0$, there exists a good stability mechanism provided by the time discretization, and thus the combination of multiple steps in the time-marching is able to enrich the contribution of the spatial DG discretization. As is shown in the above discussion, the contribution index ρ can catch up with ζ when the number of time steps m increases. Another good example is that the RKDG$(10, 4, k)$ method [11] has monotonicity stability.

5. Remarks and extensions. In this section we give some remarks and extensions for the above conclusions and/or the technique.

5.1. Discussion on combining multiple steps. We focus on the RKDG(r, r, k) method when $r \equiv 1 \pmod 4$ and $r \equiv 2 \pmod 4$. Even for combining multiple steps in the time-marching, the analysis process always shows $\zeta = \rho$ and $a^{(\zeta)}_{\zeta\zeta} > 0$. For example, when $r = 2$, for m-steps there always holds $\zeta = \rho = 2$, and

m-steps	2	3	4	5	6
$a^{(2)}_{22}$	8	48	256	1280	6144

with $\alpha_0 = 2^m$. Since all numbers are positive, we cannot claim the monotonicity stability by combining m steps. We conjecture that these RKDG schemes may not be strongly stable, and only have weak stability, for arbitrary polynomial degree k.

5.2. Lower polynomial degrees. Although monotonicity stability does not hold for arbitrary polynomial degree, it may hold if the degree is small enough when $\rho \geq 1$.

LEMMA 5.1. *There exists a constant $C > 0$ solely depending on θ, i, and μ, such that*

$$\|\partial_x^i(\mathbb{D}_\ell u^n)\| \leq \tau|\beta|\|\partial_x^{i+1}(\mathbb{D}_{\ell-1}u^n)\| + C\tau|\beta|h^{-i-1/2}\|[\![\mathbb{D}_{\ell-1}u^n]\!]\|_{\Gamma_h} \tag{5.1}$$

for any i, ℓ, and n. Here and below, ∂_x^i refers to the spatial derivative of order i.

Proof. Denote $\mathcal{S} = \mathbb{D}_\ell u^n + \tau\beta\partial_x(\mathbb{D}_{\ell-1}u^n)$. Integrating by parts yields

$$(\mathcal{S}, v) = -\tau\beta \sum_{1\leq j\leq J} [\![\mathbb{D}_{\ell-1}u^n]\!]_{j+\frac{1}{2}} \{\!\{v\}\!\}^{(1-\theta)}_{j+\frac{1}{2}} \quad \forall\, v \in V_h. \tag{5.2}$$

Taking $v = \mathcal{S}$ in (5.2) and using the inverse inequality, we have

$$(\mathcal{S}, \mathcal{S}) = -\tau\beta \sum_{1\leq j\leq J} [\![\mathbb{D}_{\ell-1}u^n]\!]_{j+\frac{1}{2}} \{\!\{\mathcal{S}\}\!\}^{(1-\theta)}_{j+\frac{1}{2}} \leq C\tau|\beta|h^{-\frac{1}{2}}\|[\![\mathbb{D}_{\ell-1}u^n]\!]\|_{\Gamma_h}\|\mathcal{S}\|, \tag{5.3}$$

which implies this lemma for $i = 0$.

Let $i \geq 1$. Taking $v = \partial_x^{2i}\mathcal{S}$ in (5.2) and integrating by parts for i times to deal with $(\mathcal{S}, \partial_x^{2i}\mathcal{S})$, we have

$$(-1)^i\|\partial_x^i\mathcal{S}\|^2 + \sum_{0\leq i'<i}\sum_{1\leq j\leq J}(-1)^{i-i'}[\![\partial_x^{i+i'}\mathcal{S}\partial_x^{i-i'-1}\mathcal{S}]\!]_{j+\frac{1}{2}} = -\tau\beta\sum_{1\leq j\leq J}[\![\mathbb{D}_{\ell-1}u^n]\!]_{j+\frac{1}{2}}\{\!\{\partial_x^{2i}\mathcal{S}\}\!\}^{(1-\theta)}_{j+\frac{1}{2}},$$

which implies, by the inverse inequality, that

$$\begin{aligned}\|\partial_x^i\mathcal{S}\|^2 &\leq Ch^{-1}\sum_{0\leq i'<i}\|\partial_x^{i+i'}\mathcal{S}\|\|\partial_x^{i-i'-1}\mathcal{S}\| + C\tau|\beta|h^{-1/2}\|[\![\mathbb{D}_{\ell-1}u^n]\!]\|_{\Gamma_h}\|\partial_x^{2i}\mathcal{S}\| \\ &\leq Ch^{-i}\|\partial_x^i\mathcal{S}\|\|\mathcal{S}\| + C\tau|\beta|h^{-1/2-i}\|[\![\mathbb{D}_{\ell-1}u^n]\!]\|_{\Gamma_h}\|\partial_x^i\mathcal{S}\|.\end{aligned}$$

Substituting the estimate of $\mathcal{S}$, we complete the proof of this lemma. ∎

As a corollary, we have the following theorem for lower order degrees.

THEOREM 5.1. *Let $\rho \geq 1$. Under the condition of Theorem* 3.1*, the RKDG(s, r, k) method has monotonicity stability for those piecewise polynomials with degree at most $\rho - 1$.*

Proof. Applying recursively Lemma 5.1, we have

$$\|\mathbb{D}_\kappa u^n\|^2 \leq C\|\partial_x^\ell(\mathbb{D}_{\kappa-\ell}u^n)\|^2 + \lambda\mathcal{Q}_3(\lambda)\tau \sum_{1\leq i\leq \ell} \|[\![\mathbb{D}_{\kappa-i}u^n]\!]\|^2_{\Gamma_h};$$

here and below $\mathcal{Q}_3(\lambda)$ is a polynomial of CFL number with nonnegative coefficients. Taking $\kappa = \ell = \rho$, we have the following conclusion:

$$\|\mathbb{D}_\rho u^n\|^2 \leq \lambda\mathcal{Q}_3(\lambda)\tau \sum_{0\leq i\leq \rho-1} \|[\![\mathbb{D}_i u^n]\!]\|^2_{\Gamma_h}$$

since the ρth order derivative in each element is zero for any polynomials of degree at most $\rho - 1$. Note that $\|\mathbb{D}_\zeta u^n\| \leq C\|\mathbb{D}_\rho u^n\|$, following from Lemma 3.4, since $\rho \leq \zeta$ and λ is smaller than 1. Hence, if the CFL number is small enough, we have $\mathcal{Y}_1 + \mathcal{Y}_2 \leq 0$, which implies monotonicity stability by substituting the above two results into (3.28). ∎

Remark 5.1. For the RKDG(r, r, k) methods with $1 \leq r \leq 12$, we list the important quantities related to their stability in the following table:

r	1	2	3	4	5	6	7	8	9	10	11	12
ζ	1	2	2	3	3	4	4	5	5	6	6	7
ρ	1	2	2	2	3	4	4	4	5	6	6	6
γ	2	4		5	6	8		9	10	12		13
k^*	0	1		1	2	3		3	4	5		5

Here k^* is the maximal degree of piecewise polynomials to achieve monotonicity stability. This result coincides with that for the RKDG(2,2,1) method in [28]. From this table, we can find out that $\zeta = \lfloor r/2 \rfloor + 1$ and $\gamma = \zeta + \rho$, where

$$\rho = \begin{cases} \zeta - 1 & \text{if } r \equiv 0 \pmod 4, \\ \zeta & \text{otherwise,} \end{cases} \tag{5.4}$$

and $\lfloor r/2 \rfloor$ is the largest integer not greater than $r/2$. In the evolution identity, we can conclude that

$$\alpha_i = \frac{1}{i!}\alpha_0, \quad 1 \leq i \leq r. \tag{5.5}$$

The above statements have been partly proved, and they will be finished in further work.

5.3. Stability by combining multiple time steps with different step sizes. The framework presented in this paper can be applied in combining multiple time steps in time-marching, even when the time step $\tau^n = t^{n+1} - t^n$ is changing. The one-step stability analysis is the same as before. However, the multistep stability analysis becomes a little more complicated. As an example, in the following we present the multistep stability analysis of the RKDG$(4, 4, k)$ scheme, which implies strong stability.

LEMMA 5.2. *Denote* $\lambda^n = |\beta|\tau^n h^{-1}$. *The RKDG(*$4, 4, k$*) scheme has two-step monotonicity stability if* λ^n *is small enough and* $\lambda^{n+1}/\lambda^n \in (0.44, 2.29)$ *holds for every* n.

Proof. Denote $\eta \equiv \tau^{n+1}/\tau^n$. The two-step time-marching can be rewritten in the form

$$(u^{n,\ell+1}, v) = \sum_{0\le\kappa\le\ell} \Big[c_{\ell\kappa}(u^{n,\kappa}, v) + d_{\ell\kappa}\tau^n \mathcal{H}(u^{n,\kappa}, v)\Big], \tag{5.6a}$$

$$(u^{n+1,\ell+1}, v) = \sum_{0\le\kappa\le\ell} \Big[c_{\ell\kappa}(u^{n+1,\kappa}, v) + \tilde{d}_{\ell\kappa}\tau^n \mathcal{H}(u^{n+1,\kappa}, v)\Big], \tag{5.6b}$$

where $\tilde{d}_{\ell\kappa} = d_{\ell\kappa}\eta$ and $\ell = 0, 1, 2, 3$. This can be looked upon as one-step time-marching of a new RKDG(8,4,k) scheme with the time step τ^n; hence the previous line of analysis still works. After defining the temporal differences, we can get the final expression

$$u^{n+2} = \sum_{0\le i\le 8} \alpha_i \widetilde{\mathbb{D}_i} u^n, \tag{5.7}$$

with the new definition of temporal differences $\widetilde{\mathbb{D}_i} u^n$ (same for $i \le 4$) and

$$\begin{aligned}\boldsymbol{\alpha} = (&576,\ 576\eta + 576,\ 288\eta^2 + 576\eta + 288,\ 96\eta^3 + 288\eta^2 + 288\eta + 96,\\ &24\eta^4 + 96\eta^3 + 144\eta^2 + 96\eta + 24,\ 24\eta^4 + 48\eta^3 + 48\eta^2 + 24\eta,\\ &12\eta^4 + 16\eta^3 + 12\eta^2,\ 4\eta^4 + 4\eta^3,\ \eta^4).\end{aligned}$$

The termination index is $\zeta = 3$, the same as that when using a fixed time step, since the matrix transferring does not affect this index that solely depends on those lower-order ($r \le 4$) temporal differences. At this moment, we have $a_{33}^{(3)} = -4608\eta^6 - 4608 < 0$ and three leading principal minors:

$$\begin{aligned}\det \mathbb{B}_0^{(3)} &= 663552\eta + 663552,\\ \det \mathbb{B}_1^{(3)} &= 36691771392\eta^4 + 146767085568\eta^3 + 220150628352\eta^2\\ &\quad + 146767085568\eta + 36691771392,\\ \det \mathbb{B}_2^{(3)} &= -169075682574336\eta^9 - 507227047723008\eta^8 + 2028908190892032\eta^6\\ &\quad + 4057816381784064\eta^5 + 4057816381784064\eta^4 + 2028908190892032\eta^3\\ &\quad - 507227047723008\eta - 169075682574336.\end{aligned}$$

To ensure all numbers are positive, it is sufficient to require $0.44 < \eta < 2.29$. This implies $\rho = 3$; hence the scheme (5.6) has monotonicity stability by Lemma 3.1. ∎

A similar but more involved discussion leads to the following conclusion.

LEMMA 5.3. *The RKDG(*$4, 4, k$*) scheme has three-step monotonicity stability if* λ^n *is small enough and* $\lambda^{n+1}/\lambda^n \in [0.5, 2]$ *holds for all* n.

As a consequence of the above two lemmas, we can conclude the stability for the RKDG$(4, 4, k)$ method.

PROPOSITION 5.1. *The RKDG(*$4, 4, k$*) scheme has strong stability for* $n \ge 2$ *if* λ^n *is small enough and* $\lambda^{n+1}/\lambda^n \in [0.5, 2]$ *holds for all* n.

Remark 5.2. Both the RKDG(8,8,k) and the RKDG(12,12,k) methods are similarly proved to have strong stability for $n \ge 2$ if λ^n is small enough, as well as $\lambda^{n+1}/\lambda^n \in [0.61, 1.65]$ and $\lambda^{n+1}/\lambda^n \in [0.70, 1.44]$, respectively, for all n.

5.4. More examples. Along the same lines of analysis, we can also obtain the L^2-norm stability for the following RKDG methods that are all cited from [11].

- The RKDG$(10, 4, k)$ method and the RKDG$(5, 3, k)$ method have monotonicity stability.
- The RKDG$(s, 1, k)$ method has weak(2) stability, and the RKDG$(s, 2, k)$ method has weak(4) stability. These results are proved for $s \leq 7$.
- The RKDG$(r + 1, r, k)$ method has the same stability as the RKDG(r, r, k) method. These results are proved for $r \leq 12$.

The detailed proof is omitted for brevity.

6. Numerical results. In this section we give some numerical examples to demonstrate our results. For simplicity, we use uniform meshes with J elements and take $\beta = 1$ in (1.1).

Example 1. First we numerically verify the stability result for the RKDG$(4, 4, k)$ method. From the previous analysis, this scheme has monotonicity stability when $k = 1$ and strong stability when $k = 2, 3$. Take $J = 16, 32, 64$, and choose the standard orthogonal basis of V_h. Then this scheme can be written in the form

$$\widetilde{\mathbf{u}}^{n+1} = \mathbb{K}\widetilde{\mathbf{u}}^n, \tag{6.1}$$

where $\mathbb{K}$ is a matrix of order $(k + 1)J$, and $\widetilde{\mathbf{u}}^n$ is a vector made up of expansion coefficients of the numerical solution u^n. The spectral norm of $\mathbb{K}^m$, denoted by $\|\mathbb{K}^m\|_2$, is equal to the L^2-norm amplification of solutions for every m steps. In Figure 1 we plot $\|\mathbb{K}^m\|_2^2 - 1$ for different CFL numbers λ, where $m = 1, 2, 3$ and $k = 1, 2, 3$. For $k = 1$ and $m = 1, 2, 3$, this quantity is always close to machine precision, which can be looked upon as zero. This shows monotonicity stability for linear piecewise polynomials. For $k = 2, 3$ and $m = 1$, this quantity strongly depends on λ, with slope 5 in the logarithmic coordinates. These two pictures at least imply weak(5)-stability for high-order piecewise polynomials. For $k = 2, 3$ and $m = 2, 3$, this quantity is also close to zero and shows m-step monotonicity stability and hence strong stability for $k = 2, 3$. These numerical results coincide with Proposition 4.4.

We also plot in Figure 2 the L^2-norm of solutions, $\|u^n\|$, for $0 \leq n \leq 12$. Here $J = 64$ and $\lambda = 0.05$, and u^0 is taken as the unit singular vector with respect to the largest singular value of $\mathbb{K}$. For $k = 1$, monotonicity stability is clearly observed. However, for $k \geq 2$, monotonicity stability does not hold at $n = 1$, and multistep monotonicity stability is observed. Hence the RKDG(4,4,k) method only has strong stability in general.

Example 2. Now we investigate the weak stability of the RKDG$(5, 5, k)$ method. As we did in the previous example, we plot in Figure 3 the quantity $\|\mathbb{K}^m\|_2^2 - 1$ for different CFL numbers λ, where $k = 2, 3, 4$ and $m = 1, 2, 3$. For $k = 2$ and $m = 1, 2, 3$, this quantity is very close to zero, which numerically verifies monotonicity stability for lower-degree piecewise polynomials. For $k = 3$ and $k = 4$, this quantity strongly depends on λ, with slope 6 in the logarithmic coordinates, for $m = 1, 2, 3$. This performance is not the same as the RKDG$(4, 4, k)$ method.

Below we would like to numerically check whether the RKDG(5,5,4) scheme is linearly unstable. To this end, the initial solution u^0 is taken as the L^2-projection of $u(x, 0) = \sqrt{2}\sin(\frac{J}{16}2\pi x)$ with $J = 16, 32, 64$. The CFL number is taken as $\lambda = 0.06, 0.08, 0.10$ since the maximal value listed in [9] is 0.115 to ensure L^2-norm stability. Notice that the results in [9] are based on Fourier eigenvalue analysis and hence are only valid for normal spatial operators, while upwind-biased DG operators are not normal. The numerical results are shown in Figure 4, where the L^2-norm of

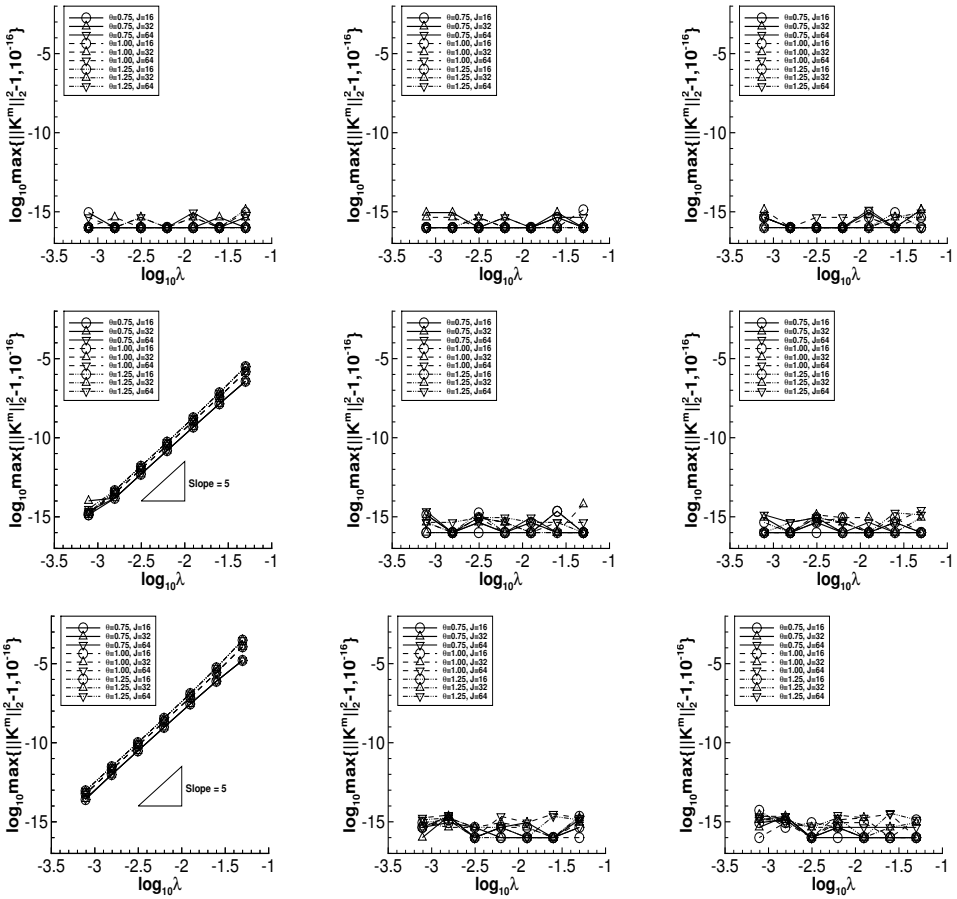

FIG. 1. *The behavior of* $\|\mathbb{K}^m\|_2^2 - 1$ *of the RKDG(*$4, 4, k$*) method for different CFL numbers* λ*:* $k = 1, 2, 3$ *from top to bottom;* $m = 1, 2, 3$ *from left to right. Here* $J = 16, 32, 64$ *and* $\theta = 0.75, 1.00, 1.25$.

the solution exponentially increases after an extremely large number of time steps (for most cases), and this phenomenon is independent of the mesh size. From the theoretical analysis in this paper, we know that the increased factor of the L^2-norm, at each time-step, is proportional to λ^6. When the CFL number is small, for example, $\lambda \leq 0.1$, this increased factor of the L^2-norm may be tiny, such that the instability phenomenon is difficult to observe numerically. This can be seen from the pictures with upwind parameters $\theta = 0.75, 1.00$. Note that the increasing of the L^2-norm becomes more serious when $\theta = 1.25$ if $\lambda \geq 0.08$.

Similar results have been observed for the RKDG$(6, 6, 4)$ method. Hence, we conjecture from our numerical experiments that the RKDG(r, r, k) method is linearly unstable for high-degree piecewise polynomials with any fixed CFL number if $r \equiv 1 \pmod 4$ or $r \equiv 2 \pmod 4$.

Example 3. Let us numerically verify strong stability for the RKDG(4,4,3) method without the same time step. To do that, we take $J = 64$ and $\tau^0 = 0.05/J$. For $n \geq 1$, we randomly take the time step $\tau^n \in [0.5\tau^0, \tau^0]$. The initial solution u^0 is taken to be the same as that in Example 1. The numerical result is plotted in Figure 5, which shows the strong stability of the scheme.

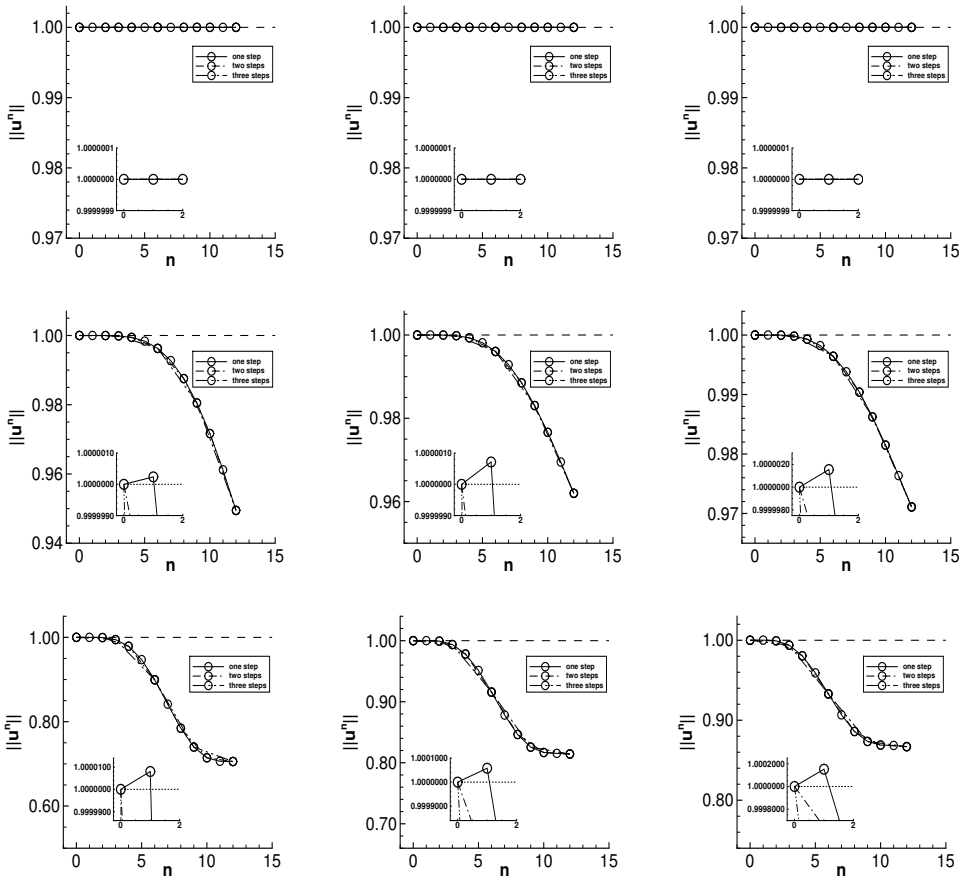

FIG. 2. *The evolution of* $\|u^n\|$ *for the RKDG(*$4, 4, k$*) method:* $k = 1, 2, 3$ *from top to bottom;* $\theta = 0.75, 1.00, 1.25$ *from left to right. Here* $J = 64$ *and* $\lambda = 0.05$.

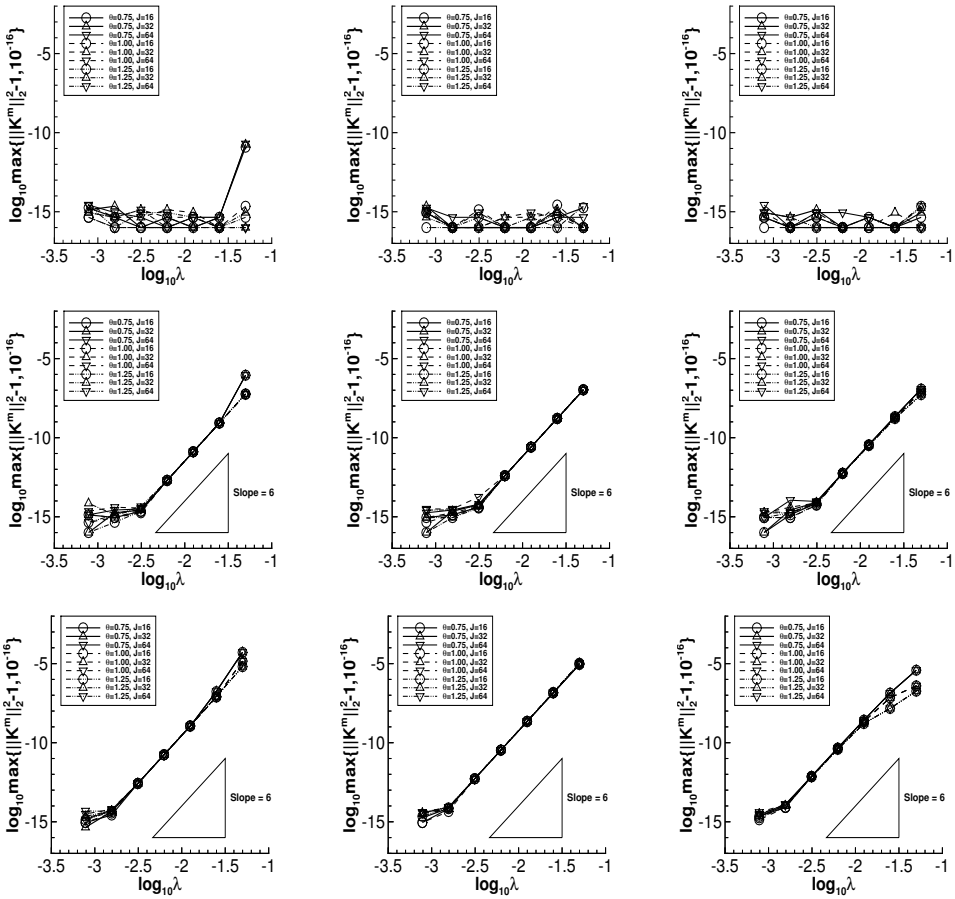

FIG. 3. *The behavior of* $\|\mathbb{K}^m\|_2^2 - 1$ *of the RKDG*$(5, 5, k)$ *method for different CFL numbers* λ*:* $k = 2, 3, 4$ *from top to bottom;* $m = 1, 2, 3$ *from left to right. Here* $J = 16, 32, 64$ *and* $\theta = 0.75, 1.00, 1.25$.

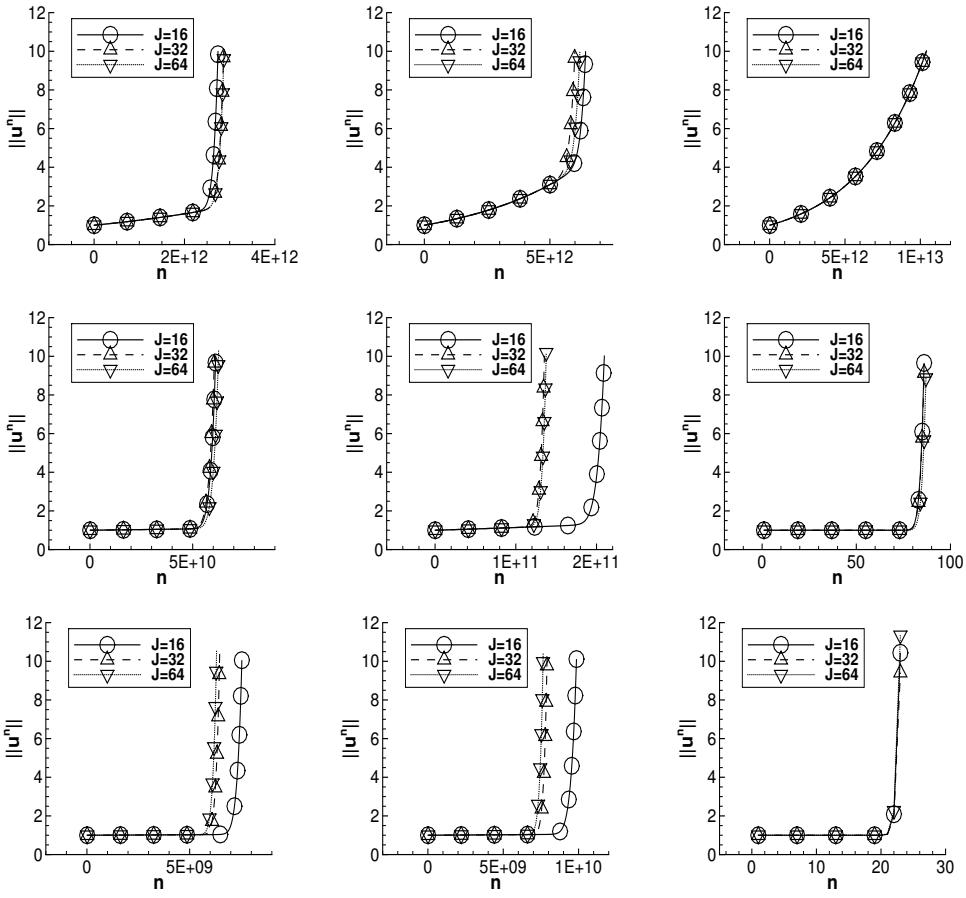

FIG. 4. *The L^2-norm of solution of the RKDG(5, 5, 4) scheme: $\lambda = 0.06, 0.08, 0.10$ from top to bottom; $\theta = 0.75, 1.00, 1.25$ from left to right. Here $J = 16, 32, 64$.*

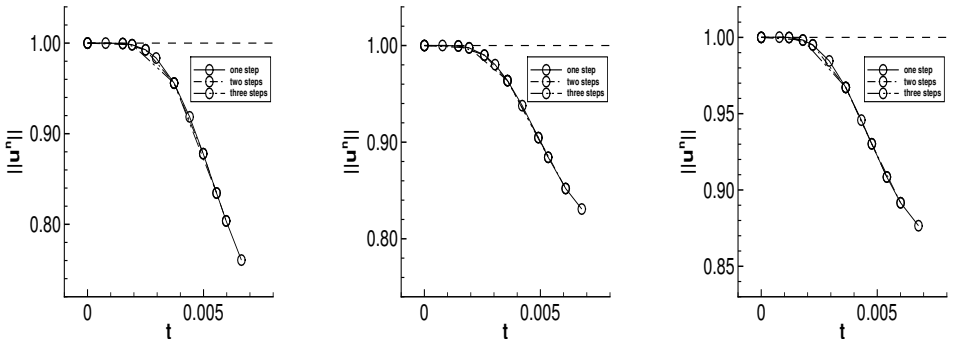

FIG. 5. *The development of $\|u^n\|$ with variable time step: RKDG(4, 4, 3), $\theta = 0.75, 1.00, 1.25$, $J = 64$, and $\lambda^0 = 0.05$, $\lambda^n \in [0.025, 0.05]$ randomly taken for $n \geq 1$.*

7. Concluding remarks. In this paper we have proposed a flexible framework to carry out the L^2-norm stability analysis for the RKDG schemes when solving linear constant-coefficient hyperbolic equations. Based on this technique, we are able to determine the different stability mechanisms and the detailed performances for many popular Runge–Kutta time-marching schemes of order up to 12. We believe that this technique can be applied to many algorithms when solving the PDEs with approximate skew-symmetric spatial discretizations. In future work, we will generalize this technique to handle multistep time-marching and apply it to hyperbolic equations with variable coefficients and nonlinear conservation laws.

REFERENCES

[1] E. Burman, A. Ern, and M. A. Fernández, *Explicit Runge–Kutta schemes and finite elements with symmetric stabilization for first-order linear PDE systems*, SIAM J. Numer. Anal., 48 (2010), pp. 2019–2042, https://doi.org/10.1137/090757940.

[2] Y. Cheng, X. Meng, and Q. Zhang, *Application of generalized Gauss-Radau projections for the local discontinuous Galerkin method for linear convection-diffusion equations*, Math. Comp., 86 (2017), pp. 1233–1267.

[3] B. Cockburn, *An introduction to the discontinuous Galerkin method for convection-dominated problems*, in Advanced Numerical Approximation of Nonlinear Hyperbolic Equations (Cetraro, 1997), Lecture Notes in Math. 1697, Springer, Berlin, 1998, pp. 15–268.

[4] B. Cockburn, S. Hou, and C.-W. Shu, *The Runge-Kutta local projection discontinuous Galerkin finite element method for conservation laws.* IV. *The multidimensional case*, Math. Comp., 54 (1990), pp. 545–581.

[5] B. Cockburn, S. Y. Lin, and C.-W. Shu, *TVB Runge-Kutta local projection discontinuous Galerkin finite element method for conservation laws.* III. *One-dimensional systems*, J. Comput. Phys., 84 (1989), pp. 90–113.

[6] B. Cockburn and C.-W. Shu, *TVB Runge-Kutta local projection discontinuous Galerkin finite element method for conservation laws.* II. *General framework*, Math. Comp., 52 (1989), pp. 411–435.

[7] B. Cockburn and C.-W. Shu, *The Runge-Kutta local projection $P1$-discontinuous-Galerkin finite element method for scalar conservation laws*, RAIRO Model. Math. Anal. Numer., 25 (1991), pp. 337–361.

[8] B. Cockburn and C.-W. Shu, *The Runge-Kutta discontinuous Galerkin method for conservation laws.* V. *Multidimensional systems*, J. Comput. Phys., 141 (1998), pp. 199–224.

[9] B. Cockburn and C.-W. Shu, *Runge-Kutta discontinuous Galerkin methods for convection-dominated problems*, J. Sci. Comput., 16 (2001), pp. 173–261.

[10] E. Deriaz, *Stability conditions for the numerical solution of convection-dominated problems with skew-symmetric discretizations*, SIAM J. Numer. Anal., 50 (2012), pp. 1058–1085, https://doi.org/10.1137/100808472.

[11] S. Gottlieb, D. I. Ketcheson, and C.-W. Shu, *High order strong stability preserving time discretizations*, J. Sci. Comput., 38 (2009), pp. 251–289.

[12] S. Gottlieb and C.-W. Shu, *Total variation diminishing Runge-Kutta schemes*, Math. Comp., 67 (1998), pp. 73–85.

[13] S. Gottlieb, C.-W. Shu, and E. Tadmor, *Strong stability-preserving high-order time discretization methods*, SIAM Rev., 43 (2001), pp. 89–112, https://doi.org/10.1137/S003614450036757X.

[14] W. Guo, X. H. Zhong, and J. M. Qiu, *Superconvergence of discontinuous Galerkin and local discontinuous Galerkin methods: Eigen-structure analysis based on Fourier approach*, J. Comput. Phys., 235 (2013), pp. 458–485.

[15] I. Harari and T. J. R. Hughes, *What are C and H?: Inequalities for the analysis and design of finite element methods*, Comput. Methods Appl. Mech. Engrg., 97 (1992), pp. 157–192.

[16] G. S. Jiang and C.-W. Shu, *On a cell entropy inequality for discontinuous Galerkin methods*, Math. Comp., 62 (1994), pp. 531–538.

[17] E. J. Kubatko, C. Dawson, and J. J. Westerink, *Time step restrictions for Runge-Kutta discontinuous Galerkin methods on triangular grids*, J. Comput. Phys., 227 (2008), pp. 9697–9710.

[18] D. Levy and E. Tadmor, *From semidiscrete to fully discrete: Stability of Runge–Kutta schemes by the energy method*, SIAM Rev., 40 (1998), pp. 40–73, https://doi.org/10.1137/S0036144597316255.

[19] Y. J. Liu, C.-W. Shu, E. Tadmor, and M. P. Zhang, *L^2 stability of the central discontinuous Galerkin method and a comparison between the central and regular discontinuous Galerkin methods*, ESAIM M2AN, 42 (2008), pp. 593–607.

[20] X. Meng, C.-W. Shu, and B. Y. Wu, *Optimal error estimates for discontinuous Galerkin methods based on upwind-biased fluxes for linear hyperbolic equations*, Math. Comp., 85 (2016), pp. 1225–1261.

[21] J. X. Qiu and Q. Zhang, *Stability, error estimate and limiters of discontinuous Galerkin methods*, in Handbook of Numerical Analysis: Basic and Fundamental Issues, Elsevier, New York, 2016, pp. 147–171.

[22] W. H. Reed and T. R. Hill, *Triangular Mesh Methods for the Neutron Transport Equation*, Los Alamos Scientific Laboratory report LA-UR-73-479, Los Alamos National Laboratory, Los Alamos, NM, 1973.

[23] C.-W. Shu and S. Osher, *Efficient implementation of essentially nonoscillatory shock-capturing schemes*, J. Comput. Phys., 77 (1988), pp. 439–471.

[24] Z. Sun and C.-W. Shu, *Stability of the fourth order Runge-Kutta method for time dependent partial differential equations*, Ann. Math. Sci. Appl., 2 (2017), pp. 255–284.

[25] Z. Sun and C.-W. Shu, *Strong stability of explicit Runge–Kutta time discretizations*, SIAM J. Numer. Anal., 57 (2019), pp. 1158–1182, https://doi.org/10.1137/18M122892X.

[26] E. Tadmor, *From semidiscrete to fully discrete: Stability of Runge–Kutta schemes by the energy method*. II, in Collected Lectures on the Preservation of Stability under Discretization (Fort Collins, CO, 2001), SIAM, Philadelphia, 2002, pp. 25–49.

[27] Q. Zhang, *Third order explicit Runge-Kutta discontinuous Galerkin method for linear conservation law with inflow boundary condition*, J. Sci. Comput., 46 (2011), pp. 294–313.

[28] Q. Zhang and C.-W. Shu, *Error estimates to smooth solutions of Runge–Kutta discontinuous Galerkin methods for scalar conservation laws*, SIAM J. Numer. Anal., 42 (2004), pp. 641–666, https://doi.org/10.1137/S0036142902404182.

[29] Q. Zhang and C.-W. Shu, *Stability analysis and a priori error estimates of the third order explicit Runge–Kutta discontinuous Galerkin method for scalar conservation laws*, SIAM J. Numer. Anal., 48 (2010), pp. 1038–1063, https://doi.org/10.1137/090771363.

[30] X. X. Zhang and C.-W. Shu, *On positive-preserving high order discontinuous Galerkin schemes for compressible Euler equations on rectangular meshes*, J. Comput. Phys., 229 (2010), pp. 8918–8934.

[31] X. H. Zhong and C.-W. Shu, *Numerical resolution of discontinuous Galerkin methods for time dependent wave equations*, Comput. Methods Appl. Mech. Engrg., 200 (2011), pp. 2814–2827.